



Evolutionary history of the sequestrate genus *Rossbeevera* (*Boletaceae*) reveals a new genus *Turmalinea* and highlights the utility of ITS minisatellite-like insertions for molecular identification

T. Orihara¹, T. Lebel², Z.-W. Ge³, M.E. Smith⁴, N. Maekawa⁵

Key words

biogeography
cryptic species
DNA barcoding
hypogeous fungi
introgression
species tree

Abstract The sequestrate (truffle-like) basidiomycete genera *Rossbeevera*, *Chamonixia*, and *Octaviana* are closely related to the epigeous mushroom genera *Leccinum* and *Leccinellum*. In order to elucidate the properties and placement of several undescribed sequestrate taxa in the group and to reveal the evolutionary history of *Rossbeevera* and its allies, we conducted phylogenetic analyses based on three nuclear (ITS, nLSU, *EF-1α*) and two mitochondrial DNA loci (*ATP6* and mtSSU) as well as precise morphological observations. Phylogenetic analyses of three nuclear loci suggest a complex evolutionary history with sequestrate fruiting bodies present in several clades, including a previously unrecognized sister clade to *Rossbeevera*. Here we propose a new sequestrate genus, *Turmalinea*, with four new species and one new subspecies as well as two new species of *Rossbeevera*. The three-locus nuclear phylogeny resolves species-level divergence within the *Rossbeevera*-*Turmalinea* lineage, whereas a separate phylogeny based on two mitochondrial genes corresponds to geographic distance within each species-level lineage and suggests incomplete lineage sorting (ILS) and gene introgression within several intraspecific lineages of *Rossbeevera*. Furthermore, topological incongruence among the three nuclear single-locus phylogenies suggests that ancient speciation within *Rossbeevera* probably involved considerable ILS. We also found an unusually long, minisatellite-like insertion within the ITS2 in all *Rossbeevera* and *Turmalinea* species. A barcode gap analysis demonstrates that the insertion is more informative for discrimination at various taxonomic levels than the rest of the ITS region and could therefore serve as a unique molecular barcode for these genera.

Article info Received: 20 February 2015; Accepted: 2 December 2015; Published: 29 February 2016.

INTRODUCTION

In recent years, molecular systematics has become increasingly popular and useful for examining the evolution of fruitbody morphology within the fleshy fungi in Ascomycota and Basidiomycota. Most types of mushroom fruitbodies, including agaricoid, gasteroid, resupinate, cup-shaped, and coralloid forms, have arisen multiple times due to convergent evolution (e.g., Hibbett et al. 1997, Bruns et al. 1998, Percudani et al. 1999, Pine et al. 1999, Peintner et al. 2001, Larsson et al. 2004, Hibbett 2004, Dentinger & McLaughlin 2006, Wilson et al. 2011, Miettinen et al. 2012). The sequestrate fruiting body form, which includes truffles, truffle-like fungi, and secotioid fungi, is characterized by fully or partially enclosed hymenia that render forcible spore discharge ineffective (Kendrick 1992). Sequestrate fungi have evolved dozens of times from other types of fruitbodies (e.g., Bruns et al. 1998, Percudani et al. 1999, Peintner et al. 2001, Læssøe & Hansen 2007, Lebel & Syme 2012; Lebel et al. 2015). Previous statistical studies suggest that evolution of the sequestrate-gasteroid form from other fruitbody forms is

irreversible (Hibbett 2004, Wilson et al. 2011), and that this evolution may offer opportunities to adopt new ecological niches (Wilson et al. 2011). Many sequestrate fungi fruit belowground (hypogeous) and produce fruitbodies that are eaten by mammals, birds, or invertebrates that facilitate spore dispersal (Fogel & Trappe 1978, Maser et al. 1978, Claridge & May 1994, Danks 2011, Beever & Lebel 2014). Animal mycophagy may also help to disperse spores directly into similar habitats with compatible mycorrhizal host plants (Frank et al. 2009, Trappe et al. 2009). Since most sequestrate fungi form mycorrhizas with plants, this animal interaction should be beneficial for efficient spore dispersal.

The *Boletaceae* is a family that primarily consists of soft-bodied, pileate-stipitate mushrooms with a poroid hymenophore (i.e., 'boletes'). In recent years, many new genera of boletes have been proposed based on multigene phylogenetic analyses of epigeous members of the *Boletaceae* (e.g., Halling et al. 2012a, b, Arora & Frank 2014, Gelardi et al. 2014, Li et al. 2014, Wu et al. 2014, Zeng et al. 2014). However, the family includes many sequestrate lineages and the number of sequestrate genera also continues to increase as more taxa are included in molecular phylogenies (Desjardin et al. 2008, 2009, Orihara et al. 2010, Trappe et al. 2013). The sequestrate genus *Rossbeevera* was erected to accommodate Australasian and Asian species of *Chamonixia* (Lebel et al. 2012a, b) that are phylogenetically close to, but distinct from, *Chamonixia* s.str. Species of *Rossbeevera* have fruitbodies with a whitish peridium that discolours bluish green to indigo and ellipsoid to fusiform basidiospores with 3–5 longitudinal ridges. Phylogenetically, this genus is part of a monophyletic lineage that also includes the epigeous bolete

¹ Kanagawa Prefectural Museum of Natural History, 499 Iryuda, Odawara-shi, Kanagawa 250-0031, Japan; corresponding author e-mail: t_orihara@nh.kanagawa-museum.jp.
² National Herbarium of Victoria, Royal Botanic Gardens Melbourne, Private Bag 2000, Birdwood Ave, South Yarra, Vic., 3141, Australia.
³ Key Laboratory for Plant Diversity and Biogeography of East Asia, Kunming Institute of Botany, Chinese Academy of Sciences, Kunming 650201, China.
⁴ Department of Plant Pathology, University of Florida, Gainesville FL 32611-0680, USA.
⁵ Fungus/Mushroom Resource and Research Center, Faculty of Agriculture, Tottori University, Tottori 680-8553, Japan.

genera *Leccinum* and *Leccinellum* and the sequestrate genera *Chamonixia* and *Octaviania* (Lebel et al. 2012a, Orihara et al. 2012b) (i.e., the ‘leccinoid clade’). *Leccinum* and *Leccinellum* are well known because many species in these genera are prized edibles collected throughout the Northern Hemisphere (but some *Leccinum* species can cause gastrointestinal distress; Bessette et al. 2000). The leccinoid clade appears particularly rich in sequestrate fungi (> 40 spp.), even when compared with other groups of Boletales with many sequestrate taxa. A total of eight *Rossbeevera* species have thus far been reported from Australia (2 spp.), New Zealand (1 sp.), Southeast Asia (1 sp.), China (2 spp.), and Japan (2 spp.) (Lebel et al. 2012a, b, Orihara et al. 2012a).

For several decades, a sequestrate fungus that is macroscopically similar to *Rossbeevera* species but with pinkish fruitbodies and ellipsoid basidiospores with 6–10 longitudinal ridges has often been collected from western Honshu, Japan. Similarly, *Rossbeevera*-like fungi with different basidiospore morphology from *Rossbeevera* have also been formally and informally reported from other areas of Japan under alternative names (i.e., *Gautieria* sp. in Aoki (1978); *Hymenogaster* sp. in Yoshimi & Doi (1989)). All of these taxa have longitudinally ridged basidiospores and in some cases exhibit a bluish discolouration that is similar to *Rossbeevera* species. In order to better assess the diversity of sequestrate fungi in the leccinoid clade, it is important to clarify the morphology and phylogeny of these poorly documented taxa.

The aim of this paper is to provide well-resolved phylogenies based on three nuclear (ITS, nLSU, *EF-1 α*) and two mitochondrial (*ATP6* and mtSSU) DNA loci (472 nucleotide sequences in total) and topological comparisons of the resultant phylogenies as well as precise morphological observations to enhance our understanding of evolution within the leccinoid clade. We include known species of *Leccinum*, *Leccinellum*, *Chamonixia*, *Octaviania*, and *Rossbeevera* as well as species that have not been formally studied in the past. Based on a combination of morphological and molecular characterization, we describe two new species of *Rossbeevera* as well as four new species and one new subspecies within the new genus *Turmalinea*. We also examine the utility of a highly divergent minisatellite-like insertion found within the ITS2 rDNA of *Rossbeevera* and *Turmalinea* spp. for molecular delimitation within the *Rossbeevera*-*Turmalinea* lineage.

MATERIALS AND METHODS

Materials examined and morphological observations

Fresh fruitbodies were collected throughout Japan and from Australia, New Zealand, and Yunnan Province, China. After morphological observation and DNA extraction, the fruitbodies were air-dried or freeze-dried for later examination. These specimens are deposited in Kanagawa Prefectural Museum of Natural History, Japan (KPM), National Museum of Nature and Science, Japan (TNS) and the Herbarium of Cryptogams, Kunming Institute of Botany, Chinese Academy of Sciences (KUN, with HKAS accession numbers). Herbarium specimens were obtained from KPM, TNS, the Oregon State University Herbarium, Oregon, USA (OSC), the Mycological Herbarium of Università degli Studi di L’Aquila, L’Aquila, Italy (AQUI), the Western Australian Herbarium (PERTH), and the National Herbarium of Victoria, Royal Botanic Gardens Victoria, Australia (MEL).

For microscopy hand-cut sections of fresh or dried specimens were mounted in water, 3 % KOH, lacto-glycerol, or 1 % phloxine B aqueous solution. To determine the amyloid reaction, dried material was stained with Melzer’s reagent. Basidiospore

dimensions (e.g., range of spore length \times spore width, length of hilar appendages) and their standard deviations (SD) were determined based on 50 measurements. The 95 % prediction intervals of basidiospore diameter are shown without parentheses in taxonomic descriptions. Both endpoints of the spore dimensions are shown in parentheses, but when the value is the same as the 95 % prediction interval, only the latter is shown. Two additional spore features are shown; the length to width ratio (Q) and the hilar appendage to spore length ratio (*HA/S*; Orihara et al. 2012a). Measurements include the hilar appendage but not spore ornamentation or the pedicel. Basidium sizes are presented as the range of the lengths \times the range of the widths. Scanning electron microscopy (SEM) was performed according to Yanaga et al. (2012).

DNA extraction, PCR amplification and sequencing

DNA was extracted from fresh or dried fruitbodies using the FTA Classic Card or Indicating FTA Cards (Whatman International Ltd, Maidstone, England) based on the manufacturer’s protocol for plants (www.whatman.com/References/WGI_1397_Plant-Poster_V6.pdf). Dried fruitbody tissues were soaked in 99.5 % ethanol for 2 min before DNA extraction according to Orihara et al. (2012a). PCR amplification of ITS, nLSU, and *EF-1 α* followed Orihara et al. (2012b) and the protocol for mtSSU was the same as for nLSU. PCR amplification of *ATP6* was performed according to Kretzer & Bruns (1999). PCR primers were ITS1F (Gardes & Bruns 1993) and ITS4 (White et al. 1990) or ITS4B (Gardes & Bruns 1993), ITS1F and ITS2, and/or ITS3 (White et al. 1990) and ITS4B for the ITS region; LR0R and LR5 (Vilgalys & Hester 1990) for the nLSU; EF1-983F and either EF1-2218R or EF1-1567R (Rehner & Buckley 2005) for *EF-1 α* ; *ATP6-3* and *ATP6-2* (Kretzer & Bruns 1999) for *ATP6*; and MS1 and MS2 (White et al. 1990) for mtSSU. Unidirectional sequencing of the PCR products in forward and reverse directions were completed according to Orihara et al. (2012b). Sequences were edited and assembled with Sequence Scanner v. 1.0 (Applied Biosystems, Foster City, California, USA), BioEdit v. 7.0.9 (Hall 1999), SeaView v. 4 (Galtier et al. 1996) and Clustal X v. 1.83 (Thompson et al. 1997). A total of 362 sequences were obtained and were deposited in the International Nucleotide Sequence Databases (INSD).

Multigene phylogenetic analyses

Specimens and sequences used for phylogenetic analyses are listed in Table 1. A total of 111 collections and 467 sequences (composed of 362 new sequences for this study and 105 sequences from INSD) were included in the multigene datasets (nuclear dataset: ITS, nLSU, *EF-1 α* ; mitochondrial dataset: *ATP6* and mtSSU). Identification of epigeous bolete taxa in the leccinoid clade that were included in the phylogenetic analyses were based not only on their sequence similarity to sequences in INSD but also on morphological descriptions by Den Bakker & Noordeloos (2005). Previous phylogenetic studies on boletoid mushrooms have shown that members of the leccinoid clade were closely related to *Austroboletus* spp., *Tylophilus virens*, *Harrya chromapes* (Binder & Hibbett 2006), *Retiboletus griseus* (Dentinger et al. 2010) or *Spongiforma thailandica* (Nuhn et al. 2013). *Spongiforma thailandica* is also closely related to *Borofutus dhakanus* and *Porphyrellus* species (Hosen et al. 2012). We therefore included taxa from all of these groups in the analyses to see which is supported as a sister to the leccinoid clade based on different loci. *Chalciporus piperatus* and *Buchwaldoboletus lignicola* were strongly supported as the earliest diverging lineage in the *Boletaceae* (Binder & Hibbett 2006, Dentinger et al. 2010, Halling et al. 2012a, b) and were therefore selected as outgroup taxa. Sequence alignments were performed using Clustal X with the data manually adjusted in SeaView v. 4.

Table 1 List of sequences used in this study. Newly generated DNA sequences are designated in **bold**. Taxa and sequences used only for the ITS analyses are indicated with asterisks (*). ITS sequence of *Rhodactina incarnata* was used only for comparison among genera.

Taxon	Locality	Voucher No.	ITS	nLSU	EF-1 α	ATP6	mtSSU
<i>Rossbeevera cryptocayana</i>	Japan, Kagoshima Pref., Amami-ohshima Isl., Yamato-son	KPM-NC 17843	-	KC552030	KC552072	KT581441	KT581442
	Japan, Kagoshima Pref., Kakeroma Isl.	KPM-NC 23928	KP222892	KP222898	KP222914	KP222885	KP222904
	Japan, Okinawa Pref., Ishigaki Isl., Eastern foot of Mt Omoto	KPM-NC 23387	KP222893	KP222899	KP222913	KP222886	KP222905
	Japan, Mie Pref., Kameyama-shi	TUMH-40255	HQ693874	HQ693879	JN378444	KC552114	KC552185
	Japan, Tottori Pref., Tottori-shi, Ouchidani (holotype)	TNS-F-36986	HQ693875	HQ693880	KC552068	KC552115	KC552186
	Japan, Tottori Pref., Tottori-shi, Ouchidani	TUMH-40252	KC551981	KC552026	KC552069	KC552116	KC552187
	Japan, Saga Pref., Nishi-matsuura-gun, Arita-cho, near the Arita Dam	TNS-F-36988	KC551982	KC552070	KC552071	KC552117	KC552188
	Japan, Okinawa Pref., Yanbaru	KPM-NC 18043	KC551983	KC552029	KC552071	KC552119	KC552190
	Japan, Kagoshima Pref., Amami-ohshima Isl., Setouchi-son	KPM-NC 23895	KP222890	KP222896	KP222915	KP222883	KP222902
	Japan, Kagoshima Pref., Amami-ohshima Isl., Amami-shi	KPM-NC 23911	KP222891	KP222897	KP222916	KP222884	KP222903
<i>Rossbeevera griseovelutina</i>	Japan, Kagoshima Pref., Amami-ohshima Isl., Yamato-son	KPM-NC 17844	KC551984	KT581439	KT581440	KC552120	KC552191
	Japan, Kagoshima Pref., Amami-ohshima Isl.	TUMH-40266	HQ693878	HQ693883	KC552073	KC552121	KC552192
	Japan, Hyogo Pref., Shiogahara	TNS-F-36990	HQ693876	HQ693881	KC552074	KC552122	KC552193
	Japan, Tottori Pref., Tottori-shi, Ouchidani	TNS-F-36992	HQ693877	HQ693882	KC552075	KC552123	KC552194
	Japan, Hyogo Pref., Shiogahara (holotype)	TNS-F-36989	KC552031	KC552076	KC552124	KC552195	KC552196
	Japan, Nagano Pref., Ida-shi, Odaira Tonge Pass, under <i>Fagus crenata</i>	KPM-NC 18094	KJ001091	KJ001101	KJ001080	KP222887	KJ001070
	Japan, Okayama Pref., Okayama Prefectural Forest Park, Bunanodaira, under <i>Fagus crenata</i>	TNS-F-36991	KC551985	KC552032	KC552077	KC552125	KC552196
	Japan, Kanagawa Pref., Odawara-shi, Inyuda, near Myoriki-ji temple, under <i>Castanopsis cuspidata</i>	KPM-NC 18044	KC551986	KC552033	KJ001081	KJ001066	KC552197
	Japan, Ehime Pref., Tobe-cho, Sasadani, under <i>Quercus acutissima</i>	KPM-NC 17734	KJ001093*	-	-	-	-
	New Zealand, NZ South Isl., Te Anau Valley, Fiordland Nat. Park, Greebe Saddle.	MEL 2079341	KC551974	KC552021	-	KC552104	KC552175
<i>Rossbeevera pachydermis</i>	New Zealand, NZ South Isl., Te Anau to Milford Sound Rd, The Chasm trail	MEL 2079350	HQ647138	HQ647157	-	-	-
	New Zealand, NZ North Isl., Te Urewera National Park, Aniwanui, Black Beech Track, under <i>Nothofagus</i> trees	KPM-NC 23334	KJ001087	KJ001094	KJ001076	-	-
	New Zealand, NZ North Isl., Te Urewera National Park, Aniwanui, Track to Lake Wakareiti, under <i>Nothofagus</i> trees	KPM-NC 23336	KJ001088	KJ001095	KP222912	KJ001064	KJ001072
	New Zealand, NZ North Isl., Matawai, Te Wera Reserve (Matawai Conservation Area), under <i>Nothofagus</i> trees	KPM-NC 23347	KJ001089	KJ001096	KJ001077	KP222881	KJ001073
	New Zealand	PDD 89084	GU22301*	-	-	-	-
	Japan, Nara Pref., Nara Park, under <i>Quercus gilva</i>	KPM-NC 17847	KC551987	KC552034	KC552078	KC552126	KC552198
	Japan, Nara Pref., near Mt Kasuga, under <i>Q. gilva</i>	KPM-NC 18023	KC551988	KC552035	-	-	-
	Japan, Nara Pref., near Mt Kasuga, under <i>Q. gilva</i>	KPM-NC 18087	KJ001086	KJ001100	KJ001082	KJ001068	KJ001071
	Japan, Osaka Pref., Minoh-shi, Mt Minoh, in a <i>Castanopsis</i> -evergreen <i>Quercus</i> forest	KPM-NC 17848	KC551989	KC552036	KC552079	KC552127	KC552200
	Japan, Nara Pref., near Mt Kasuga, under <i>Q. gilva</i>	KPM-NC 23940	KP222894*	-	-	-	-
<i>Rossbeevera paracyanea</i> *	Victoria, Eastern Highlands region	A.W. Claridge 2137	-	KC552022	KC552063	KC552105	KC552176
	Victoria, Gippsland region	A.W. Claridge 2785	-	KC552023	KC552064	KC552106	KC552177
	Australia, Tasmania, Mount Field, Lyrebird Track, Mt Field Nat. Park.	MEL 2078292	-	KC552024	KP222910	KC552107	KC552178
	Australia, Victoria, East Gippsland, Erinundra National Park, along Orbst-Bendoc Rd.	TO-AUS-72	KC551977	KC552025	KC552065	KC552108	KC552179
	Australia, Victoria, Midlands, Langi Ghiran (Forest Park) edge of picnic area	MEL 2329434	KJ001084	KJ001097	KJ001075	KJ001065	KJ001074
	Australia, Victoria, Snowfields, Mount Buffalo	MEL 2321058	KJ001085	KP222895	KP222911	KP222882	KP222901
	Australia, South Australia, Nangwary, Nangwary Forest Reserve, South western island Swamp, J. Packer, 22 July 2009 (AD56098)	AD56098 (TLe846)	KC551975*	-	-	-	-
	Australia, New South Wales, Genoa National Park	OSC61484	KC551976	JN378506	JN378446	KC552109	KC552180
	Australia, New South Wales, c. 5 km south of the junction between Princess highway and Eden rd.	TO-AUS-46	KC551978	JN378507	JN378447	KC552110	KC552181
	<i>Rossbeevera vittatispora</i> *	Australia, Western Australia, Beedelup National Park, Anzac Rd.	OSC61480	KC551979	JN378505	JN378445	KC552111
Australia, WA, Darling, Dryandra, Tomingley Rd under <i>Allocasuarina</i> .		MEL 2219011	KC551980	HQ647161	KC552066	KC552112	KC552183
Australia, WA, Darling, Jarrahdale Rd., under <i>Casuarina fraseriana</i> and <i>Eucalyptus marginata</i>		MEL 2322708	-	HQ647160	KC552067	KC552113	KC552184

Table 1 (cont.)

Taxon	Locality	Voucher No.	ITS	nLSU	EF-1 α	ATP6	mtSSU
<i>Rosbeeveria yunnanensis</i>	China, Yunnan Prov., Chu Xiang Pref., Mt Zi Xi	KPM-NC 17850	KC551990	JN979437	KC552080	KC552128	KC552201
<i>Turmalinea chrysocarpa</i>	China, Yunnan Province, Manhao, Gejiu, alt. 860 m, in a broad-leaf forest.	HKAS 70601 (Ge3098)	KC552003	KC552051	–	KP222888	KC552216
<i>Turmalinea mesomorpha</i> subsp. <i>mesomorpha</i>	Japan, Aomori Pref., Towada, Ohoronai	KPM-NC 18012	KC551999	KC552047	KC552090	KC552139	KC552212
	Japan, Iwate Pref., Appi-Kogen	KPM-NC 18014	KC552000	KC552048	KC552091	KC552140	KC552213
	Japan, Aomori Pref., Towada, Tsuta-onsen	KPM-NC 18059	KJ001090	KJ001099	–	KJ001067	KJ001069
<i>Turmalinea mesomorpha</i> subsp. <i>sordida</i>	Japan, Ehime Pref., Saijo-shi, Mt Ishizuchi, in a <i>Fagus crenata</i> forest.	KPM-NC 18016	KC552001	KC552049	KC552092	KC552141	KC552214
	Japan, Ehime Pref., Matsuyama-shi, Mt Takanawa, under <i>F. crenata</i>	KPM-NC 17743	KC552002	KC552050	KJ001078	KC552142	KC552215
	Japan, Mie Pref., Kameyama-shi	KPM-NC 17856	–	KC552037	KC552081	KC552129	KC552202
<i>Turmalinea persicina</i>	Japan, Kyoto Pref., Sakyo-ku, Iwakura-agura-cho	KPM-NC 18001	KC551991	KC552038	KC552082	KC552130	KC552203
	Japan, Kyoto Pref., Higashiyama-ku, Kiyomizu Shirime	KPM-NC 17858	KC551992	KC552039	KC552083	KC552131	KC552204
	Japan, Hiroshima Pref., Hiroshima-shi, Higashi-ku, Hiroshima Prefecture Ryokka-Center	KPM-NC 18003	KC551993	KC552040	KC552084	KC552132	KC552205
	Japan, Nara Pref., Nara-shi, Mt Kasuga	KPM-NC 18004	KC551994	KC552041	KC552085	KC552133	KC552206
	Japan, Oita Pref., Saiki-shi, Shiroyama Park	KPM-NC 18006	KC551995	KC552042	KC552086	KC552134	KC552207
	Japan, Oita Pref., Saiki-shi, Nakayama, Shirohachiman-Shrine	KPM-NC 18007	–	KC552043	KC552087	KC552135	KC552208
	Japan, Oita Pref., Saiki-shi, Ume-Oh-aza, Shigeoka, 1.3 km southwest of Sotaro Station	KPM-NC 18008	KC551996	KC552044	KC552088	KC552136	KC552209
	Japan, Hyogo Pref., Shiogahara	KPM-NC 18053	KC551997	KC552045	–	KC552137	KC552210
	Japan	Muroi361	–	DQ218598	DQ219224	DQ218885	DQ218741
<i>Turmalinea yuwanensis</i>	Japan, Kagoshima Pref., Amami-Oshima Isl.	KPM-NC 18011	KC551998	KC552046	KC552089	KC552138	KC552211
	Japan, Okinawa Pref., Takashiki-jima Isl.	KPM-NC 23377	KJ001092	KJ001098	KJ001083	KP222889	KP222906
<i>Chamonixia caespitosa</i>	USA (locality of the ATP6 sequence is unknown.)	p6931 (ATP6: F-945)	EU669385	EU669427	–	AF114444	AF213145
	USA (ITS & nLSU); Canada, New Brunswick, Fundy Natural Park, Point Wolfe (mtSSU)	p0711	EU669208	EU669260	–	–	–
<i>Leccinellum crocipodium</i>	France	930809/1; RC.F94.103 (ITS)	JN21053	AF139693	KF030434	–	–
<i>Leccinellum aff. crocipodium</i>	Japan, Tottori Pref., Yazu-cho, Hatto	KPM-NC 18041	KC552053	KC552054	KC552165	KC552166	KC552240
<i>Leccinellum aff. griseum</i>	Japan, Hyogo Pref., Uwano	KPM-NC 17831	KC552008	JN378508	JN378449	KC552163	KC552238
	Japan, Tottori Pref., Tottori-shi, Ouchidani	HKAS 50221	–	JN378509	JN378450	KC552164	KC552239
<i>Leccinellum</i> sp.	China	HKAS 50221	–	–	–	–	–
<i>Leccinellum 'albellum'</i>	USA, NY, Erie County	MB06-040	–	–	–	–	–
<i>Leccinellum aff. duriusculum</i>	Japan, Hyogo Pref., Uwano	KPM-NC 17830	KC552009	JN378510	JN378448	KC552166	KC552241
	Japan, Tottori Pref., Tottori-shi, Mt Ohginosen	KPM-NC 18034	KC552010	KC552054	KC552095	KC552167	KC552242
<i>Leccinellum scabrum</i>	Austria	Ls1	–	AF139705	–	–	–
<i>Leccinellum scabrum</i>	UK, Scotland, Aberdeenshire, Burn O' Vat	KPM-NC 17840	KC552012	JN378515	JN378455	KC552170	KC552245
<i>Leccinellum aff. schistophilum</i>	Japan, Hyogo Pref., Uwano	KPM-NC 17841	KC552011	KC552055	KC552096	KC552168	KC552243
<i>Leccinellum</i> sp.	Japan, Iwate Pref., Appi-Kogen	KPM-NC 17839	–	JN378513	JN378453	KC552169	KC552244
<i>Leccinellum versipelle</i>	UK, Scotland, Denmet Oakwood National Nature Reserve	KPM-NC 17833	–	JN378514	JN378454	KC552172	KC552247
<i>Leccinellum vulpinum</i>	UK, Scotland, Aberdeenshire, near Mar Lodge Estate	KPM-NC 17834	KC552013	JN378516	JN378456	KC552171	KC552246
<i>Octaviania arbutalensis</i>	Spain	CJ0121111NR02	–	KF14252	–	–	–
<i>Octaviania asahimontana</i>	Japan, Hokkaido, Kamikawa-cho, Mt Daisetsu	KPM-NC 17824	–	JQ619178	JN378489	KC552154	KC552228
<i>Octaviania asterosperma</i>	Spain, Sella Covallera	Trappe 23377	–	JN257998	JN378497	KC552158	KC552233
	Italy, Provincia L'Aquila, Comune di Cappadocia	AQU1 3899	–	KC552052	KC552093	KC552159	KC552234
<i>Octaviania celatiffia</i>	Japan, Nara Pref., Nara-shi, Nara Park - Mt Kasuga	KPM-NC 17776;	JN257997	KP222900	JN378416	KC552147	KC552221
	KPM-NC 18082 (nLSU)	–	–	–	–	–	–
<i>Octaviania cyanescens</i>	OR, Lane Co., Lanb Butte south of English Mountain.	PNW FUNGI 15603	KC552006	JN378502	JN378438	KC552160	KC552235
<i>Octaviania decimae</i>	Japan, Kyoto Pref., Mt Hiei	KPM-NC 17763	JN257991	JN378465	JN378409	KC552145	KC552219
<i>Octaviania durianelloloides</i>	Japan, Kanagawa Pref., Minami-ashigara-shi	KPM-NC 17829	–	–	–	–	–
<i>Octaviania etchuensis</i>	Japan, Toyama Pref., Nakashingawa-gun, Teteiyama-cho	KPM-NC 17822	–	–	–	–	–
<i>Octaviania hesperi</i>	Japan, Kanagawa Pref., Zushi-shi	KPM-NC 17793	–	–	–	–	–
<i>Octaviania japonimontana</i>	Japan, Akita Pref., near Lake Towada	KPM-NC 17797	–	–	–	–	–
<i>Octaviania kobayasi</i>	Japan, Nara Pref., Nara-shi, Mt Kasuga	KPM-NC 17785	–	–	–	–	–
	Japan, Kyoto Pref., Uji-shi	KPM-NC 17783	–	–	–	–	–
<i>Octaviania mortae</i>	Japan, Tottori Pref., Hie Shirine	KPM-NC 17770	–	–	–	–	–
<i>Octaviania nonae</i>	Japan, Kagoshima Pref., Amami-oshima Isl.	KPM-NC 17748	–	–	–	–	–

<i>Octaviania nonae</i>	Japan, Hyogo Pref., Shiohahara	KPM-NC 17751	JN257988	JN378462	JN378406	KC552144	KC552218
<i>Octaviania tasmanica</i>	Australia, Tasmania, Mount Field, Mt Field Nat. Park.	MEL 2341996	KC552004	JN378495	JN378436	KC552156	KC552231
	Australia, NSW, Southern Tablelands, off Nungatta Rd.	MEL 2128484	KC552005	JN378496	JN378437	KC552157	KC552232
<i>Octaviania yaeyamaensis</i>	Japan, Okinawa Pref., Ishigaki Isl., Mt Omoto	KPM-NC 17819	JQ619180	JN378491	JN378432		
<i>Octaviania zelleri</i>	USA, Maine, Tunk Lake, off route 182	MES270		JN378498	JN378440	KC552161	KC552236
<i>Aureoboletus thibetanus</i>	China	HKAS 41551 (AFTOL-ID450)	DQ200917	AY700189	DQ029199		
<i>Austroboletus occidentalis</i>	Australia, Victoria, Aire River Crossing, Otways National Park	CD587		KC552061	KC552102		
<i>Austroboletus</i> sp. 1	Australia, Victoria, On Quarry Track off Wannan Diversion Track about midway between Wannan Diversion Track and quarry	MEL 2053830	KC552016	KC552058	KC552099		
<i>Austroboletus</i> sp. 1	Australia, Tasmania, Peter Murrell Nature Reserve, Site HEB, (55G, 524413, 5238290)	MEL 2300518	KC552017	KC552059	KC552100		
<i>Austroboletus</i> sp. 2	Australia, Victoria, Colac Otway Shire, Carlisle State Park, Cricket Pitch Track, 7.5 km W Gellibrand	MEL 2265009	KC552015	KC552057	KC552098		
<i>Austroboletus</i> sp. 3	Australia, Western Australia, Walpole - Normalup National Park, the Knoll lower walk	MEL 2233764	KC552014	KC552056	KC552097		
<i>Austroboletus</i> sp. 4	New Caledonia, Southern Province, Thio to Nagety Road, 26 km north of Thio	MEL 2305143	KC552018	KC552060	KC552101		
<i>Boletellus projectellus</i>	USA, MA	MB 03-118	AY789082	AY684158	AY879116		
<i>Borofutus dhakanus</i>	Bangladesh, Dhaka Division, Gazipur, Bhawal National Park	HKAS 73792	JQ928607	JQ928617	JQ928575		
<i>Buchwaldoboletus lignicola</i>	Germany, Maindreieck	Pu11		JQ326997	JQ327040		
<i>Chalciporus piperatus</i>	USA, MA, Rutland State Park	MB 04-001		DQ534648	GU187690		
<i>Harrya chromapes</i>	Japan, Tottori Pref., Yazu-cho	KPM-NC 17835	KC552019	JN378517	JN378457	KC552173	KC552249
<i>Porphyrellus porphyrosporus</i>	Germany, Walhalla, Bavaria	MB 97-023	DQ534563	DQ534643	GU187734		
<i>Retiboletus griseus</i>	USA, VA, George Washington National Forest, Shenandoah Mountain (LSU sequence); NY (<i>EF-1α</i> sequence)	BD210 (LSU), Both sn (<i>EF-1α</i>)			HQ161858		
<i>Retiboletus</i> aff. <i>griseus</i>	China	HKAS59460	JQ928613	JQ928626	JQ928580		
<i>Rhodactina incarnata</i>	Thailand, Chang Mai, Sanpatong District, Mae Wang Conservation Forest, Sanpatong-Ban Guard Road	OSC 130505	KC552020*				
<i>Spongiforma thailandica</i>	Thailand, Nakorn Nayok Province, Khao Yai National Park	DED 7873	EU685113	EU685108	KF030436		
<i>Tylopius virens</i>	Japan, Kanagawa Pref., Odawara-shi, Iryuda	KPM-NC 18054		KC552062	KC552103	KC552174	KC552250

For testing topological congruence among different loci, we directly compared statistically supported topologies (BS \geq 75 %) in ML trees constructed with RAXML v. 7.2.6 (Stamatakis 2006), setting the number of bootstrap replicates to 1 000. Introns of *EF-1 α* were carefully adjusted in SeaView and also included in the analyses. Approximately 80 % of nucleotides were invariable in the mtSSU dataset and we therefore included only 106 bp of variable sites in the phylogenetic analyses.

In the ITS dataset, a large part of the ITS1 and ITS2 regions were too divergent to be aligned across the leccinoid clade and the allied taxa. Therefore, we first tested whether to include unambiguously aligned sites using the Gblocks algorithm (Castresana 2000) in SeaView v. 4. This allowed smaller final blocks, gap positions within the final blocks, and less strict flanking positions. The resultant dataset was 263 bp in length and many phylogenetically informative positions that contained gaps were excluded from the analysis based on the results produced by Gblocks. Consequently, the ML tree generated from the dataset by RAXML was poorly resolved with evidence of long-branch attraction of *B. dhakanus* and *S. thailandica* within the *Leccinum* clade. Because of these inconsistent results we abandoned the Gblocks dataset and manually and carefully selected phylogenetically informative sites within ITS using SeaView, allowing inclusion of the sites that contained gaps (up to approximately 40 % of the individuals at any given site). The final ITS dataset for the multi-locus analyses was 462 bp in length, and the resultant ML tree had much higher resolution without obvious evidence of long-branch attraction.

Subsequently, two multigene datasets that consisted of three nuclear (i.e., ITS, nLSU, and *EF-1 α*) and two mitochondrial (i.e., *ATP6* and mtSSU) DNA loci, respectively, were created to examine the phylogeny of the leccinoid clade and to check for topological incompatibility between nuclear and mitochondrial phylogenies. In both datasets, we included only specimens with sequences for at least two loci (i.e., specimens represented by only ITS were omitted in the nuclear dataset; Table 1). Gaps were treated as 'missing' data for all analyses. The nuclear and mitochondrial combined datasets are deposited in TreeBASE (accession URL: <http://purl.org/phylo/treebase/phyloids/study/TB2:S15097>).

For each dataset, Bayesian analysis was conducted with MrBayes 3.2 (Ronquist & Huelsenbeck 2003). The combined dataset was partitioned by regions for the non-coding sequences and by codons for the coding sequences, and the best-fit likelihood models were estimated for the resultant 10 partitions with MrModeltest 2.3 (Nylander 2004). The GTR+I+G model was used for all the nuclear partitions (i.e., ITS1-5.8S-ITS2, nLSU, and the 1st, 2nd, and 3rd codons and introns of *EF-1 α*) and the 1st and 3rd codons of *ATP6*, the GTR+G model for mtSSU, and the F81 model for the 2nd codon of *ATP6*. Bayesian posterior probabilities (PP) were approximated by the Metropolis-coupled Markov chain Monte Carlo method (Geyer 1991). Two parallel runs were conducted with one cold and seven heated chains each for 10M generations, starting with a random tree. The parameter for temperature of the seven heated chains in both runs was set to 0.10. Trees were saved to a file every 1 000th generation. We determined that the two runs reached convergence when the average SD of split frequencies (ASDSF) continuously dropped below 0.01. We further verified the convergence by checking that the effective sample size (ESS) of each resulting statistic was sufficiently large (> 200) using Tracer v. 1.6 (Rambaut & Drummond 2009). Trees obtained before reaching convergence were discarded as the burn-in, and the remaining trees were used to calculate a 50 % majority consensus topology and to determine PP values for individual branches.

The same combined datasets were also analysed by the maximum likelihood (ML) method with raxmlGUI 1.3 (Silvestro & Michalak 2012), which includes executable files of RAXML 7.4.2 (Stamatakis 2006). The best-fit ML tree was inferred under the GTR+I+G model. The datasets were partitioned in the same way as in the Bayesian analysis so that different α -shape parameters, GTR rates, and empirical base frequencies could be assigned to each partition. To check statistical support for the resultant tree topology, the rapid bootstrap (BS) option was used under the automatically assigned GTR+CAT model, setting the number of replicates to 1 000.

Species tree analyses

Since several topological conflicts were found among individual single-locus nuclear phylogenies, we conducted species tree estimation from gene trees using *BEAST program (Heled & Drummond 2010) in the software package BEAST 2 v. 2.1.3 (Bouckaert et al. 2014) to see whether the multi-locus combined phylogeny conflicts with the species phylogeny based on a multispecies coalescent model. *BEAST estimates a Bayesian species tree from the simultaneously generated, individual gene trees, and reconstructs a species phylogeny that reflects the effect of incomplete lineage sorting (ILS) or deep coalescence (Heled & Drummond 2010). In the *BEAST analysis we excluded species with any missing loci from the analysis because they could negatively effect the MCMC convergence (Castillo-Ramírez et al. 2010). Thus, we were not able to include *Austroboletus* cf. *novae-zelandiae*, *Buchwaldoboletus lignicola*, *Chalciporus piperatus*, *Leccinum 'albellum'*, *Leccinum* sp., *L. versipelle*, *Octaviania arbutalensis*, *O. asterosperma*, *O. zelleri*, *Retiboletus griseus*, '*Turmalinea chrysocarpa*', and *Tylophilus virens*. For the other species we included specimens with sequences of all the three loci. Consequently, the concatenated nuclear datasets consisted of 78 sequences, which were grouped into 43 species according to the results of the ITS, nLSU, and *EF-1 α* analyses. The dataset was partitioned into ITS, nLSU, and *EF-1 α* regions.

XML command files for executing *BEAST analysis was created using BEAUti in the BEAST 2 package. Substitution models for each locus were estimated with MrModeltest: the HKY+I+G model was assigned to the non-partitioned *EF-1 α* dataset whereas the GTR+I+G model was used for the ITS and nLSU datasets. The number of rate categories for the discrete gamma model was set to four according to Yang (1994), and 'piecewise linear and constant root' was applied to the species tree population size model. In the Bayesian MCMC prior settings, gamma distribution was applied to mutation rates and clock rates for each dataset. Both the analyses were run for 200M generations, storing an inferred tree in every 10 000 generations. The other settings were left at defaults. The runs were monitored using Tracer v. 1.6 to verify the convergence of the MCMC by checking that the ESS of each resulting statistic was sufficiently large (> 100). The output data were summarized using TreeAnnotator in the BEAST 2 package. The resulting trees were viewed with FigTree v. 1.4. (<http://tree.bio.ed.ac.uk/software/figtree/>).

Detection and characterization of insertion sequences within ITS2

The full-length ITS dataset (3' end of SSU-ITS1-5.8S-ITS2-5' end of LSU) of the *Rossbeevera* and *Turmalinea* species consisted of 51 sequences. The dataset was not properly aligned by the automatic alignment with ClustalX v. 1.83 or with Q-INS-I option in MAFFT v. 7 (Katoh & Standley 2013) due to highly divergent sequences with indels and unusually long insertions within ITS. We therefore aligned the dataset manually with SeaView. The dataset is deposited in TreeBASE

(accession URL: <http://purl.org/phylo/treebase/phylows/study/TB2:S15097>). Internal, discontinuous repeats within the ITS region were detected with the aid of dot plot matrices generated with the BLASTN search using the default settings (Altschul et al. 1997). The search of more-or-less regular, continuous, ITS tandem repeats was implemented with Tandem Repeats Finder software v. 4.04 (Benson 1999) under the following parameter settings: match = 2, mismatch = 3, indel = 5, minimum alignment score to report repeat = 50, and maximum period size = 300. In one case the analysis detected both a single nucleotide motif and the repeated pattern that consisted of the same core motif and its successive duplication as 'consensus patterns' (i.e., both 'TTTGCA' and 'TTTGCATTGCA'). In that case, we counted only the single nucleotide motif as a detected consensus pattern (i.e., 'TTTGCA' in the above example). After careful alignment of the dataset, the boundaries of the insertions were determined based on the results of BLASTN searches and Tandem Repeats Finder analyses.

To assess the usefulness of the ITS2 insertion for taxonomic identification, we implemented barcode gap analysis using the web version of the ABGD (Automatic Barcode Gap Discovery) software, which was primarily designed to delimit species from unexplored groups of metazoans (Puillandre et al. 2012). ABGD detects gaps between the infraspecific and interspecific divergence based on a matrix of pairwise distances and groups the input sequences into several hypothetical species. The largest gap is initially detected with various prior limits of maximal distance of infraspecific divergence (P), so that the dataset is partitioned according to the gap. The gap detection is iterated within each recursive partition until 'large gaps' are no longer found under the parameter P and X , where X is a proxy for minimal gap width (Puillandre et al. 2012). The analysis was performed using the default settings (i.e., $P_{min} = 0.001$, $P_{max} = 0.1$, $X = 1.5$) except the number of steps for P and for a distance-distribution histogram were set to 100 and 60, respectively. The web version of ABGD provides three distance models for the analysis: Jukes-Cantor, the Kimura's two-parameter, and simple distances. Accordingly, we chose the Kimura's two-parameter model (Kimura 1980; $Ti/Tv = 0.9059$ in the ITS2 insertion dataset; 1.2955 in the residual ITS dataset excluded the insertion sequences), which had a higher likelihood score than the Jukes-Cantor model based on model estimations in MrModeltest 2.3. In addition, ML analysis of the ITS2 insertion dataset was implemented using RAXML under the GTR+I model, which was chosen as the best model in MrModeltest 2.3, and rapid bootstrap analysis was carried out in the same settings as those of combined datasets described above.

RESULTS

Topological incongruence among different single-locus datasets

Prior to multi-locus analyses, we first examined topological congruency among three nuclear-locus trees (ITS, nLSU, and *EF-1 α*) and among two mitochondrial-locus trees (*ATP6* and *mtSSU*) separately. The resulting tree topology in the ITS, nLSU, and *EF-1 α* datasets showed conflicts in the branching order within the *Rossbeevera* clade (Fig. 1; entire trees not shown). Maddison & Knowles (2006) suggest that including more individuals and more loci reduces the effect of incomplete lineage sorting and contributes to reconstructing a more accurate species tree. Since all of the species in this clade contain multiple individuals, we concatenated the datasets for the following analyses and carefully compared the resultant multi-locus phylogeny with a species tree inferred from the three single-locus Bayesian phylogenies by using *BEAST. In contrast to the nuclear dataset, there was no obvious conflict

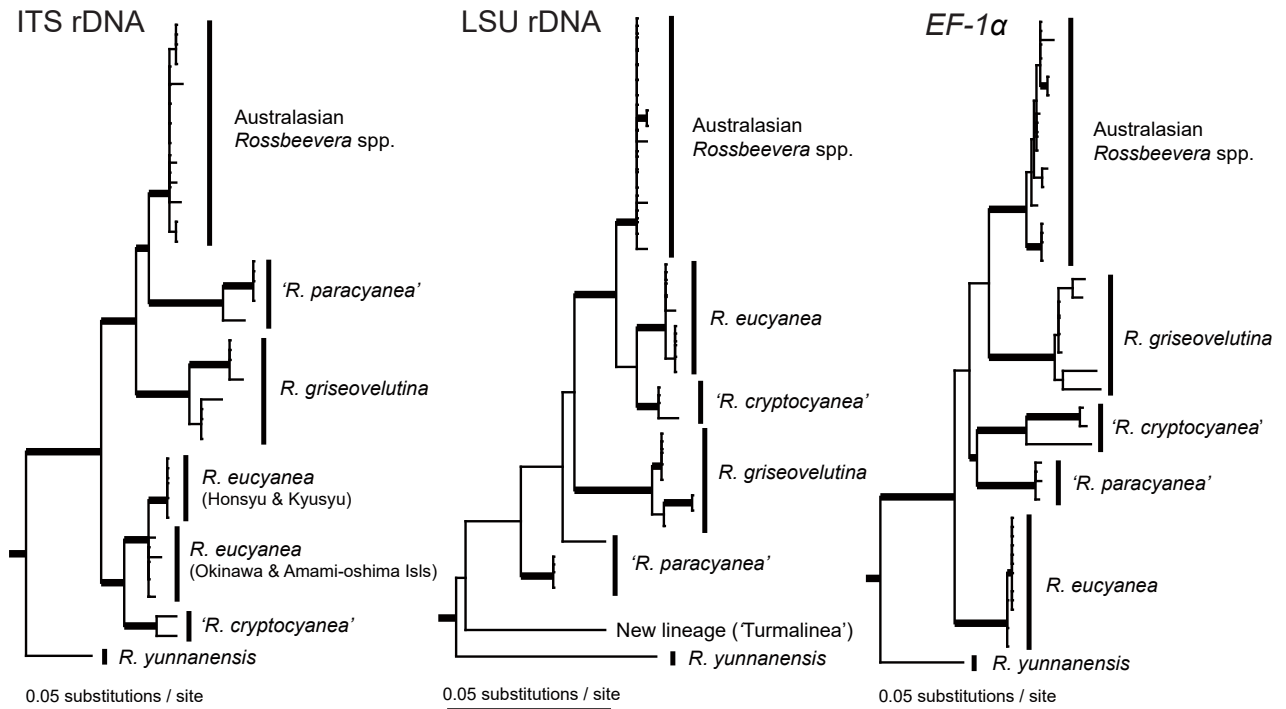


Fig. 1 Comparison of maximum likelihood (ML) tree topologies of three nuclear-locus phylogenies (ITS, nLSU, and *EF-1α*) of *Rossbeevera*. Branches supported by RAxML bootstrap (BS) values $\geq 75\%$ (1 000 replicates) are shown as thickened lines. Names with dashes represent the lineages that have not been reported in previous studies.

between the mitochondrial *ATP6* and mtSSU phylogenies, partly due to poor resolution of the mtSSU phylogeny.

Although most of the species represented by multiple individuals formed monophyletic clades in the three nuclear datasets, we found topological discordance in the relationship in *Octaviania* subg. *Parcaea*, which resulted in collapse of the monophyly of the species-level clades. That is, in the nLSU phylogeny the *O. nonae* sequences showed paraphyly with *O. celatifilia*. This topology is documented in Orihara et al. (2012b) and has only a minor influence on the phylogenetic relationships of *Rossbeevera* and its relatives, which are the focus of this study. Thus, we retained the sequences in the combined dataset.

Species tree and multi-locus combined tree based on the nuclear datasets

Since topological discordance among the three nuclear phylogenies was observed in the *Rossbeevera* clade (Fig. 1), we first inferred a species tree from Bayesian ITS, nLSU, and *EF-1α* 'gene' trees using *BEAST and subsequently compared the topology with the multi-gene tree based on the concatenated dataset. In the *BEAST analysis, all the parameters reached plateau before 5M generations. We therefore discarded the first 500 species trees as burn-in and summarized the remaining 19 501 trees for the PP calculation. ESS values of all the parameters became sufficiently large (> 100) after 200M generations. The average Log Likelihood (ln L) of the sampled species trees was 19 907.124.

The combined dataset of three nuclear loci (i.e., ITS and LSU rDNA, and *EF-1α*) consisted of 110 individuals and 2 586 base pairs. In the Bayesian inference, the ASDSF of the two parallel MCMC runs dropped constantly below 0.01 after c. 2.15M generations. Thus, the first 2 150 trees in each run were discarded as burn-in according to the ASDSF value, and the remaining 15 702 trees (sampled from 7.85M generations) were used to calculate a 50% majority consensus tree and determine PPs. ESSs of all the parameters were sufficiently large. Total arithmetic mean and harmonic mean of Likelihoods (ln L) were $-23\,076.11$ and $-23\,171.84$, respectively. The maximum likeli-

hood analysis resulted in one ML tree (ln L = $-22\,947.590387$). Overall tree topologies between the Bayesian and ML trees were almost identical, and no topological conflict was observed. The resultant topology recovered a strongly supported leccinoid clade (BS = 100%, PP = 1.00) that included *Chamonixia*, *Leccinum*, *Leccinellum*, *Octaviania* and its three subgenera, *Rossbeevera*, and a novel sequestrate lineage sister to *Rossbeevera* (Fig. 3) (i.e., *Turmalinea*).

Although there were some taxa omitted in the *BEAST species tree, overall topologies of the species tree and three-locus combined tree were similar (Fig. 2, 3). There was no strong topological conflict found between the two phylogenies. Both phylogenies showed that the novel *Turmalinea* clade was monophyletic and sister to *Rossbeevera* spp. In the *BEAST species tree the new lineage '*R. cryptocyanea*' was shown to be a sister to *R. eucyanea* with strong statistical support despite the topological inconsistency among the single nuclear gene trees. However, the other infrageneric conflicting topologies among the gene trees were not resolved in the species tree analysis although they were resolved in the multigene combined analyses with relatively high statistical support. We therefore refrain from highlighting these infrageneric relationships here and will discuss it in more detail below.

In the Bayesian and ML combined phylogenies, every genus and subgenus in the leccinoid clade except *Leccinellum* was strongly supported as monophyletic by both BS and PP (Fig. 3). The novel *Turmalinea* clade contains four undescribed sequestrate species and two subspecies from Japan and China. All of the lineages were strongly supported by both BS and PP (BS $\geq 89\%$, PP = 1.00). In the *Rossbeevera* clade, two unknown species-level lineages were nested within the clade; *Rossbeevera cryptocyanea* sp. nov. and *R. paracyanea* sp. nov., both of which are morphologically similar to *R. eucyanea* and are distributed in Japan.

The sequestrate genus *Chamonixia* was recovered as the earliest diverging lineage within the leccinoid clade with moderate statistical supports (Fig. 3). The sister lineage to the leccinoid clade was not resolved in our analyses. A sequestrate species,

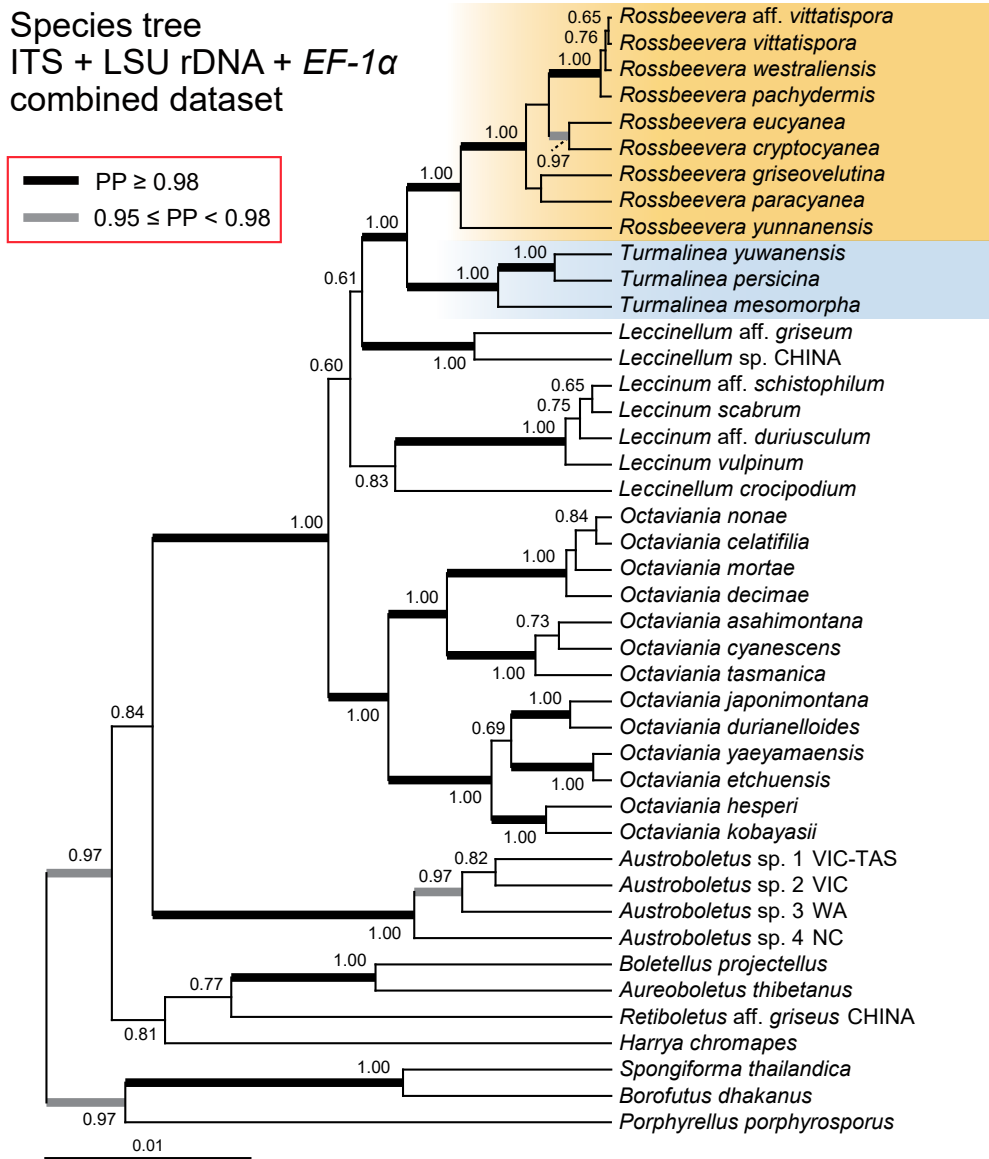


Fig. 2 Bayesian species tree inferred based on three nuclear loci (ITS, nLSU, and *EF-1α*) using BEAST. A total of 78 individuals with sequence data of all three loci were grouped into 43 terminal species-level taxa. Bayesian posterior probabilities (PP) are indicated above or below branches. Branches strongly supported by PP are highlighted as thickened lines.

Spongiforma thailandica, that was formerly supported to form a monophyletic clade with *R. griseus* and *Leccinum* spp. (Nuhn et al. 2013), formed a strongly supported monophyletic clade with *Borofutus dhakanus* and *Porphyrellus porphyrosporus* as shown in Hosen et al. (2012). Consequently, a recently proposed subfamily *Leccinoideae*, which includes *Retiboletus*, *Borofutus*, and *Spongiforma* as well as the genera in the leccinoid clade (Wu et al. 2014), was not recovered in our nuclear multi-locus analyses.

Mitochondrial multi-locus phylogeny of the Leccinoid clade

The two-locus mitochondrial dataset (i.e., *ATP6* and SSU mtDNA) consisted of 85 specimens and was 840 bp in length. In the Bayesian inference, the ASDAF of the two parallel MCMC runs dropped constantly below 0.01 after c. 1.77M generations. Thus, the first 1 770 trees in each run were discarded as burn-in, and the remaining 16 462 trees (sampled from 8.23M generations) were used to calculate a 50 % majority consensus tree and determine PPs. ESS values of all the parameters were sufficiently large (> 200). Total arithmetic mean and harmonic mean of Likelihoods (ln L) were $-3\ 541.11$ and $-3\ 614.29$, respectively. The ln L of the resultant ML tree in the RAXML



analysis was $-3\ 431.324125$. Monophyly of *Leccinum*, *Rossbeevera*, the *Turmalinea* clade, and the three *Octaviania* subgenera were recovered with varying statistical support (Fig. 4). However, most basal topologies, including relationships of the three *Octaviania* subgenera, were not resolved or were poorly supported.

Topological comparison between the nuclear and mitochondrial phylogenies

We examined topological differences between nuclear and mitochondrial phylogenies (Fig. 3, 4) and compared the resultant topologies of the *Rossbeevera-Turmalinea* lineage to determine whether there were any discrepancies in patterns of divergence (Fig. 5). The nuclear phylogeny based on the combined dataset of ITS, LSU, and *EF-1α* had high resolution and generally showed infraspecific divergence with strong statistical support regardless of the geographic distribution of the samples. For example, sequences of *R. griseovelutina*, '*R. paracyanea*' and '*R. cryptocyanea*' diverged into two strongly supported infraspecific lineages (lineages 1 and 2 in each species; Fig. 5). However, we did not find evidence of any obvious biogeographic disjunction within these species nor did we detect distinct mor-

Nuclear phylogeny
ITS + LSU rDNA + *EF-1 α*
combined dataset

— PP \geq 0.98 & MLBS \geq 70 %
— PP \geq 0.98 & MLBS < 70 %

 Boletoid (pileate-stipitate)
 Sequestrate (truffle-like)

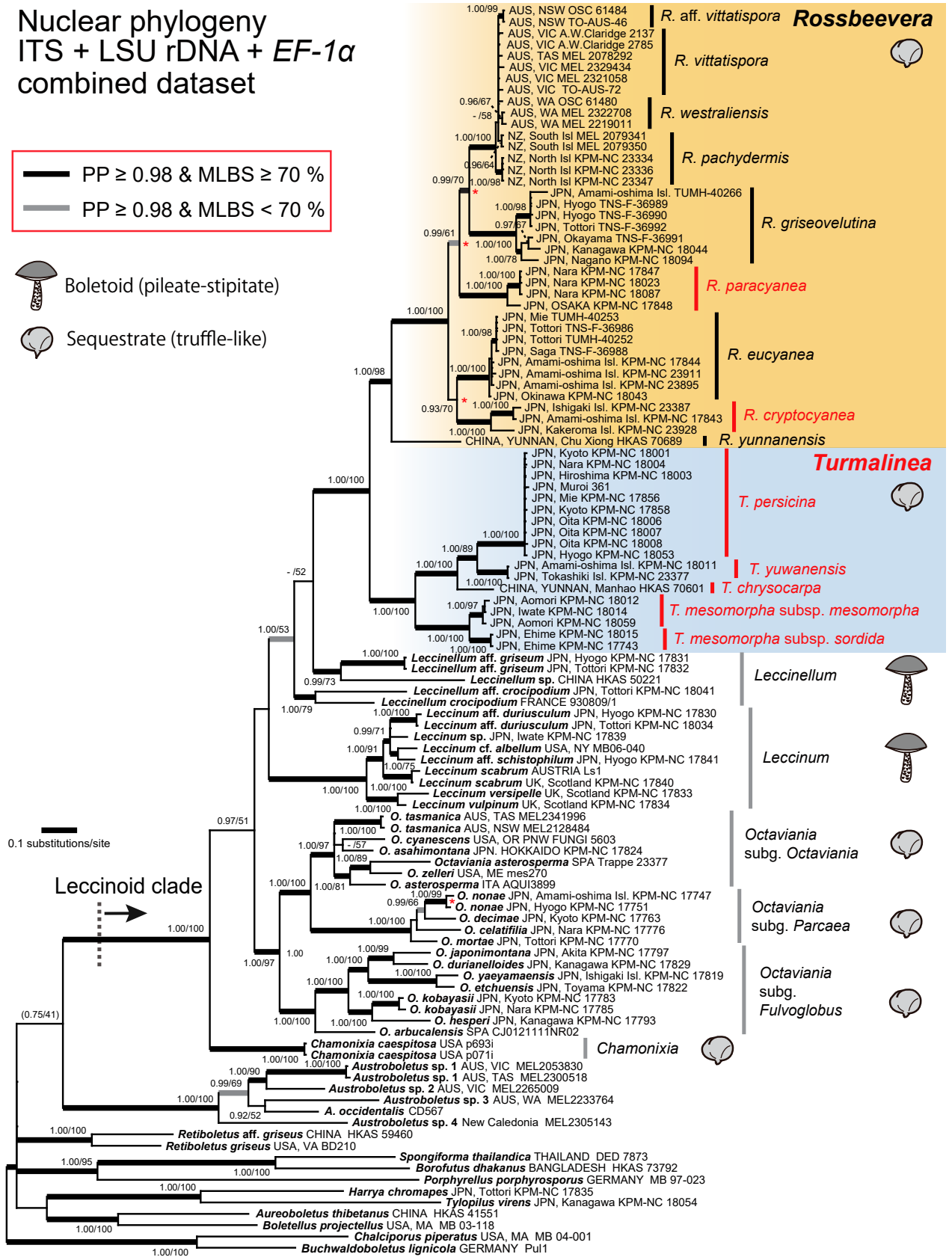


Fig. 3 Bayesian 50 % majority-rule consensus tree of the nuclear three-locus dataset (ITS, nLSU, and *EF-1 α*) of *Rossbeevera* and allied genera (i.e., the leccinoid clade). Bayesian PP and RAXML bootstrap (BS) values (1 000 replicates) are indicated above or below branches or at nodes as PP/BS. Values of PP < 0.90 or BS < 50 % are not shown. Branches supported by both PP \geq 0.98 and BS \geq 70 % are depicted as thickened black lines. Branches supported by both PP \geq 0.98 and BS < 70 % are shown as thickened grey lines. Incompatible topologies between the combined phylogeny and nuclear single-locus phylogenies are indicated by red asterisks. Names of new taxa and new lineages are coloured in red. *Chalciporus piperatus* and *Buchwaldobolletus lignicola* were used as outgroups.

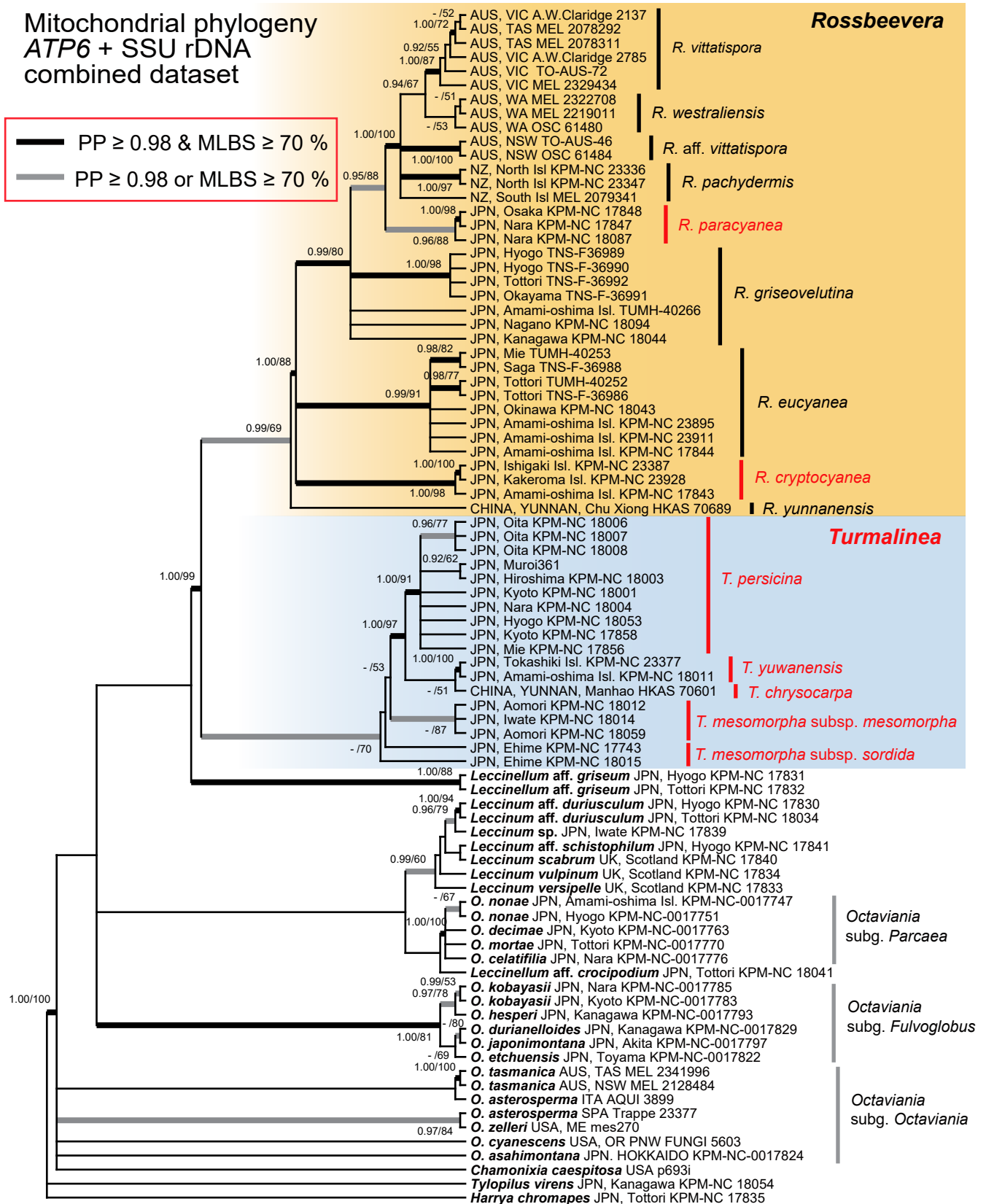


Fig. 4 Cladogram of Bayesian 50 % majority-rule consensus phylogeny of the mitochondrial two-locus dataset (*ATP6* and *mtSSU*). Bayesian PP and RAXML BS are indicated at nodes as PP/BS. Values of PP < 0.90 or BS < 50 % are not shown. Branches supported by both PP ≥ 0.98 and BS ≥ 70 % are depicted as thickened black lines. Branches supported by either PP ≥ 0.98 or BS ≥ 70 % are shown as thickened grey lines. Names of new taxa and new lineages are coloured in red.

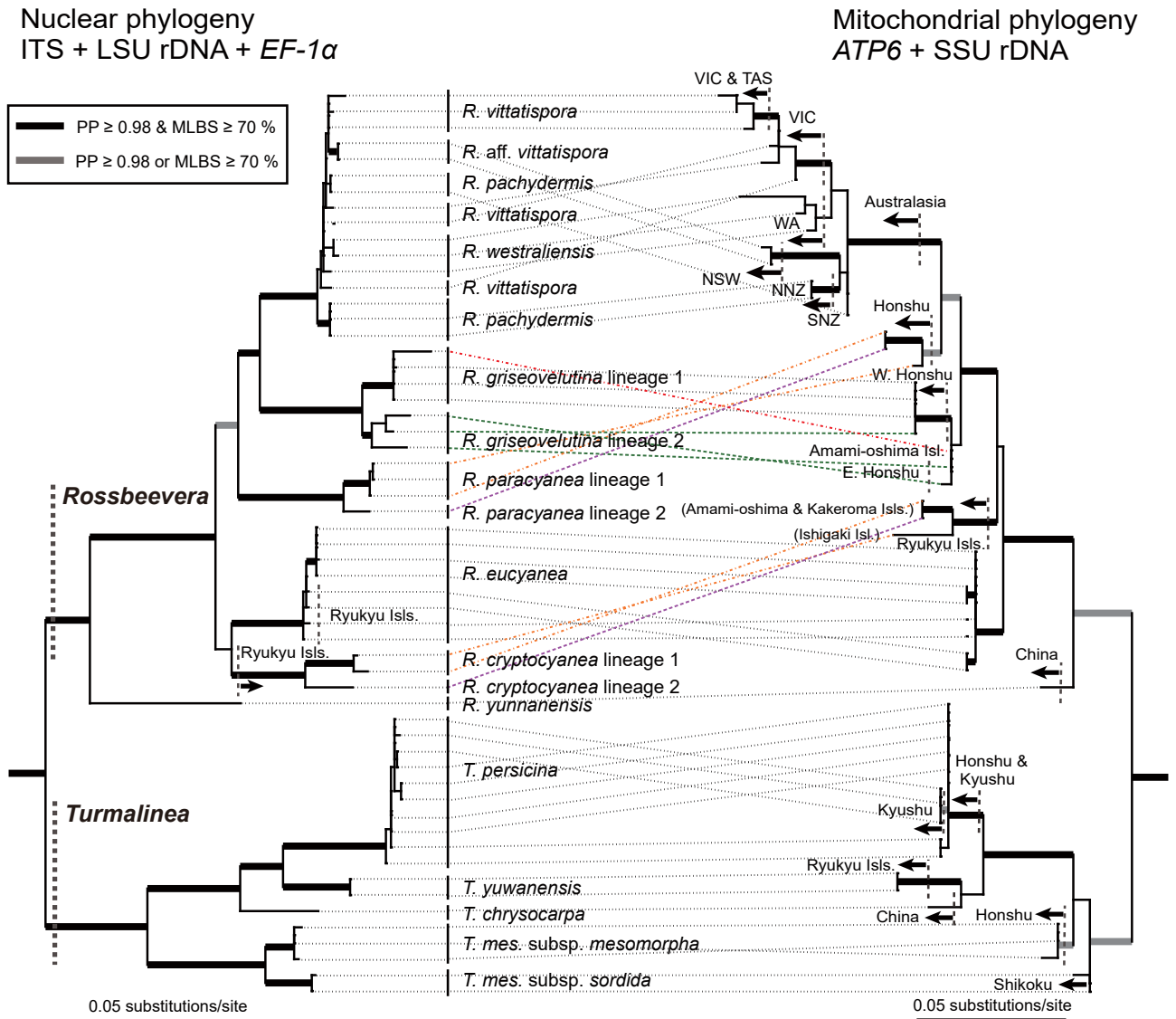


Fig. 5 Comparison of nuclear three-locus (ITS, nLSU, and *EF-1 α* ; left) and mitochondrial two-locus (*ATP6* and mtSSU; right) ML topologies of the *Rossbeevera* and *Turmalinea* clade. Bayesian PP and RAxML BS are indicated at nodes as PP/BS. Values of PP < 0.90 or BS < 50 % are not shown. The collection localities are indicated on branches of either the nuclear or mitochondrial phylogenies. Location data are as follows: TAS = Tasmania, VIC = Victoria, WA = Western Australia, NSW = New South Wales, NNZ = North Island, New Zealand, SNZ = South Island, New Zealand, W = Western, E = Eastern.

phological differences between the infraspecific lineages. Little divergence was recognized within Australasian *Rossbeevera* lineages, at least at the species level, despite the different morphologies and distributions of the described species. On the other hand, the mitochondrial phylogeny had relatively poor resolution and also generally reflected differences in distribution within each species shown in the nuclear phylogeny. Within the terminal Australasian *Rossbeevera* clade, we noted distinct divergence between the nuclear and the mitochondrial datasets. The mitochondrial topology of the clade was concordant with distributional patterns rather than morphological circumscription proposed by Lebel et al. (2012a) although some branches were not statistically supported (Fig. 5). For example, specimens that were morphologically identified as *R. vittatispora* were remarkably divergent in the mitochondrial dataset, but clearly reflected geographical proximity between Tasmania and Victoria. In the mitochondrial phylogeny, one individual of the '*R. paracyanea*' lineage 1 (KPM-NC 18087) was divergent from the '*R. paracyanea*' lineage 2, whereas another individual of the '*R. paracyanea*' lineage 1 (i.e., KPM-NC 17847) was identical to the '*R. paracyanea*' lineage 2. A very similar pattern was observed between '*R. cryptocyanea*' lineages 1 and 2, although they also exhibited geographical proximity among the specimens in the mitochondrial phylogeny (i.e., Kakeroma Island is

separated from Amami-oshima Island only by a narrow strait and they belong to the same group of islands, whereas Ishigaki Island is about 650 km distant from Amami-oshima).

Characterization of a minisatellite-like insertion within *ITS2*

We found that species of *Rossbeevera* and the *Turmalinea* clade have an unusually long insertion with indistinct tandem repeats within their *ITS2* rDNA region. The inserted sequences ranged in size from 199 to 603 bp (Table 2). The Tandem Repeats Finder analysis detected one or two continuous tandem repeats in the *ITS2* of 12 of 16 lineages of the clade (Table 2). Most of the detected tandem repeats contained a common GAGTGAAAGTG motif or similar derivative sequences. This core pattern and the derivatives scattered within insertions of every lineage in the group. In addition, one terminal lineage of the *Turmalinea* clade (i.e., '*T. persicina*') had another highly conserved core motif, AATTTAATTATTGGTGTGGAAGCTTGATTGTAAA, which is 34 bp in size and appeared three times just after the 3'-end of the GAGTGAAAGTG core pattern in the insertion. *Turmalinea persicina* is divided into two slightly divergent infraspecific groups (Fig. 6c). The copy number of the continuous motifs detected by the Tandem Repeats Finder analysis ranged from 1.9 to 5.9 (Table 2).

Table 2 Characterization of the minisatellite-like insertions within the ITS2 region of *Rossbeevera* and '*Turmalinea*' spp. Only consensus patterns with alignment score ≥ 50 are shown. Two slightly divergent intraspecific lineages of '*T. persicina*' were analysed independently. N.D. = not detected.

Taxon	Nos. of sequences examined	Insertion size (bp)	Nucleotide similarity within each lineage	Tandem repeats information					
				Consensus pattern of tandem repeats (size (bp))	Copy number	Percent of matches	Percent of indels	Score	Entropy (0–2)
<i>R. cryptocyanea</i>	2	362–366	94 %	TAGTAAAGGCATTAGTAATGGAAGCTTGAGTGAAAAAGTGAGAATGTA (48)	2.1	84	12	158	1.76
<i>R. eucyanea</i>	8	319–324	> 98 %	TGCAACACAGCTGAAAAAGCATTAGTAATGGAAGCTCCTGAGTGAAAAAGTGAGCCCATGGTATACCC ATGGTAGAATGAAAGCTTTGAGTGAAAGTGAGGATGTAGTAAAGGCTTGGAAAGCCATAGTCATT GAAAAAGCTAGTTAAACAAGGAATTTGAAAAAACAAG (169)	1.9	80	9	465	1.88
<i>R. griseovelutina</i>	8	339–344	> 96 %	AAAAGCATAGTAATGAAAACTCGAGTGAAAGTGAAAAATGGTGTA (46)	2	79	10	130	1.79
<i>R. pachydermis</i>	5	223–224	100 %	N.D.	N.D.	N.D.	N.D.	N.D.	N.D.
<i>R. paracyanea-1</i>	3	309	100 %	N.D.	N.D.	N.D.	N.D.	N.D.	N.D.
<i>R. paracyanea-2</i>	2	326	100 %	N.D.	N.D.	N.D.	N.D.	N.D.	N.D.
<i>R. vittatispora</i>	4	334–340	98 %	ATTTCTATGTCATACGGCTGAAAAGCATTAGTAATGGAAGCTTGAGCGGAAAGTAAACTATGTGAT AAAAGGCATAGTAAAGGTAAAGCTTGAGTGAAAGTGAGATGGAAGTGAGTAGGGCTGGAAGCATAG CATTAGAAAAGCTAGTAAAAAGGAATTTGAAAAAATAACCTGTGGAAT (178)	1.9	78	10	476	1.88
<i>R. aff. vittatispora</i>	2	341	99 %	N.D.	N.D.	N.D.	N.D.	N.D.	N.D.
<i>R. westraliensis</i>	2	335–337	99 %	ATTTCTATGTCATACGGCTGAAAAGCATTAGTAATGGAAGCTTGAGCGGAAAGTAAACTATGTGAT AAAAGGCATAGTAAAGGTAAAGCTTGAGTGAAAGTGAGATGGAAGCTGGAAGCCGATAG TCATTAGAAAAGCTAGTAAAAAGGAATTTGAAAAAATAACCTGTGGAAT (179)	1.9	80	7	502	1.88
<i>R. yunnanensis</i>	1	199	N/A	TATGTGTAAAAAGCATTAGTAATGGAAGCTTTGAGTGAAAGTGAGGATGTA (52) GTGAAAGTGAGCTATGA (17)	4	69	18	199	1.81
<i>T. chrysocarpa</i>	1	397	N/A	AGTAAAAAGCTATGTGAATAGGCTAGGGTACAGTAAGCTGGAAGCATAGTATGGAAGCTAGAAAG (66) AAAGTGGAAATTTGAATGATTGGACGGGAAAGCTCGAGGTG (39)	2	81	4	196	1.89
<i>T. mes. subsp. mesomorpha</i>	3	400	100 %	TGAAAAGCTCTAAG (13) AATTTAATGAATGGCGTGGAAAGCTCGAAGTG (31)	2.1	74	5	83	1.82
<i>T. mes. subsp. sordida</i>	2	395	100 %	TGAAAAGCTCTAAG (13) AATTTAATGAACGGCGATGGAAAGCTCGAGTG (31)	2.4	88	0	52	1.91
<i>T. persicina-1</i>	4	600–601	> 99 %	TIATTTGGTGGAAAGCTTGAGGGGAAAGTACTAATTTAA (38) TGGAAAGCATACTGAGTGAAGCTAG (25)	5.9	53	15	145	1.85
<i>T. persicina-2</i>	3	603	> 99 %	GGAAGCTTGAGGGAAAGACTAGTTAATGGA (31) TGGAAAGCATACTGAGTGAAGCTAG (25)	2.1	78	15	69	1.86
<i>T. yunnanensis</i>	2	272–273	> 99 %	TGAAAAGCCTAAGTGAAGAT (19) TAGAGTAAAAAGAGCTAATG (20)	2.2	79	12	55	1.81
					2.1	70	4	51	1.84

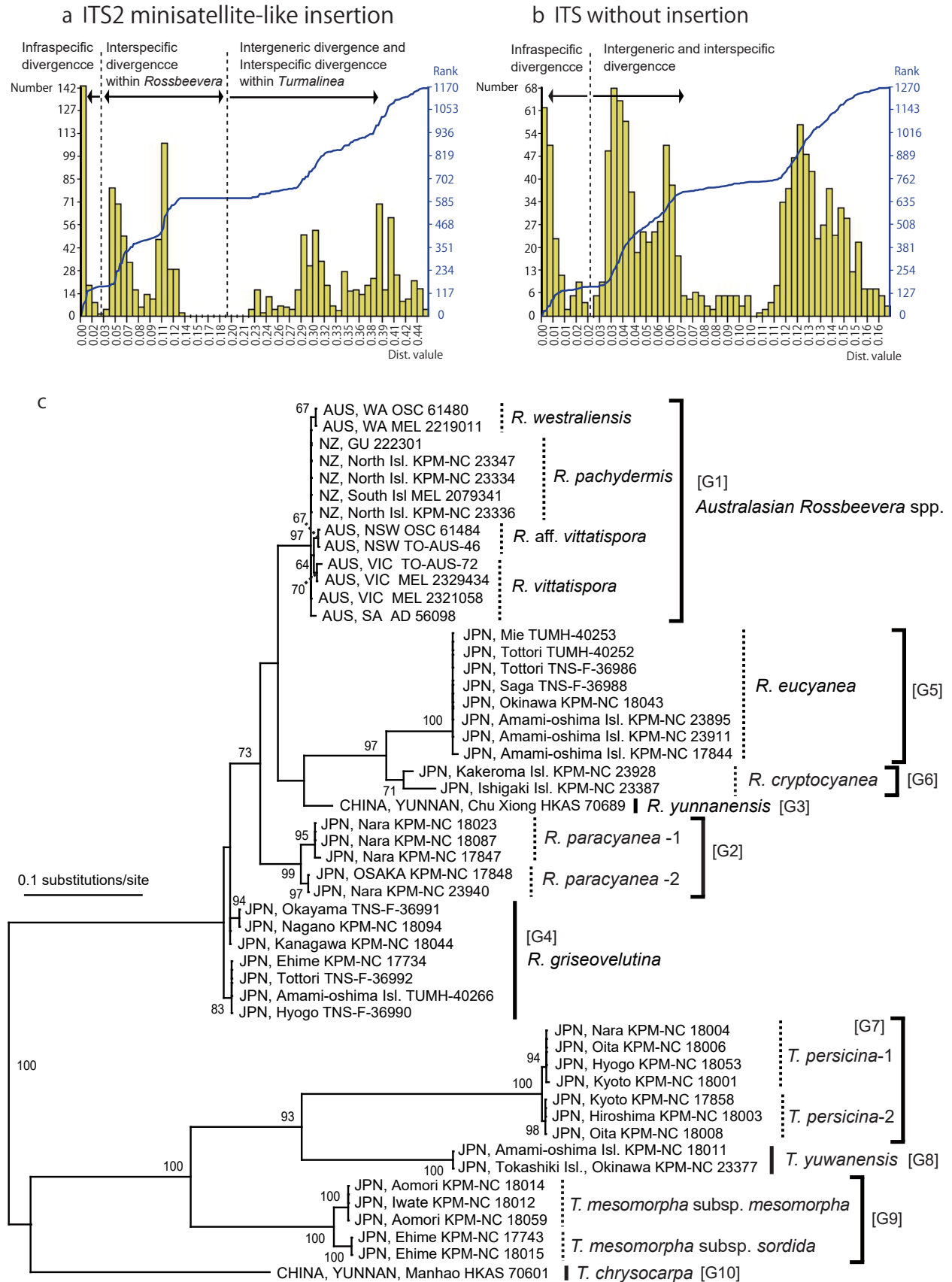


Fig. 6 Barcode gap analysis and ML phylogeny of minisatellite-like insertion within the nuclear ITS2 rDNA of *Rossbeevera* and the *Turmalinea* clade. – a. Results of the Automatic Barcode Gap Discovery (ABGD) analysis of the minisatellite-like insertion dataset. The dataset is composed of 51 sequences and is 838 nucleotides in length. Histogram of genetic distances between sequences and cumulative frequency of the distance value (ranked value; indicated as the blue line) in the distance matrix are shown. The ‘barcode gaps’ are represented as horizontal lines on the ranked value. – b. Results of the ABGD analysis using the ITS dataset excluding the minisatellite-like regions. The dataset is composed of the same individuals as ‘a’ and is 668 nucleotides in length. – c. ML phylogeny based on the same insertion dataset as ‘a’. 10 species-level groups recovered with prior intraspecific divergence $0.019 \leq P \leq 0.038$ in ABGD are designated onto the phylogeny as [G1] – [G10]. These partitions correspond to the boundary of interspecific divergence designated in ‘a’. Two intraspecific groups of *T. persicina* are identical to those in Table 1. The RAxML bootstrap (BS) value (1 000 replicates) is indicated above or below branches (only BS values $\geq 50\%$ are shown).

The minisatellite-like insertions found in every species of the *Rossbeevera-Turmalinea* lineage were highly conserved within each species (and infraspecific lineage) but highly divergent between species or genera (Table 2). Furthermore, the barcode gap analysis showed that the minisatellite sequence region can be used to delimit the boundary between intergeneric-level, interspecific-level, and infraspecific-level divergence more distinctly than the rest of the ITS region (Fig. 6a, b). The boundary between infra- and interspecific-level divergence is supposed to be present at $0.0025 < D < 0.003$, where D is a genetic distance value of pairwise distances in a dataset (Fig. 6a). The minisatellite dataset was both primarily and recursively partitioned into the ten species-level clusters already represented in Fig. 3, 5 with $0.019 \leq P \leq 0.038$ in the recursive partitions, where P is a prior limit of maximal distance of infraspecific divergence (Fig. 6c). As in the other nuclear analyses, Australasian *Rossbeevera* spp. were not very divergent and this species-complex was not partitioned at the species-level genetic boundary estimated by the barcode gap analysis. Also, there was a distinct difference in interspecific genetic distance within *Rossbeevera* and within *Turmalinea* in the minisatellite dataset, while the difference was unclear in the rest of the ITS region (Fig. 6a, b).

The ITS2 minisatellite ML phylogeny mostly recovered monophyly of the *Rossbeevera* and *Turmalinea* species represented in the other phylogenies in this study (Fig. 6c; $\ln L = -2\ 615.994733$). The monophyly of *R. griseovelutina* was not supported in the ML phylogeny of the minisatellite-like insertion within the nuclear ITS2 rDNA, probably due to the effect of the long genetic distance between the *Rossbeevera* and *Turmalinea* clades. The infraspecific divergence within '*R. paracyanea*', *R. griseovelutina*, '*T. persicina*', and '*T. mesomorpha*' was strongly supported in the analysis. Contrary to the pattern found in species of the *Rossbeevera-Turmalinea* lineage, the sister taxon of this group, *Leccinellum griseum* (= *L. pseudoscabrum*), had only a single 111 bp insertion in the ITS 2 region and Tandem Repeats Finder analysis did not detect any repeating motifs in this DNA fragment.

Taxonomy

The phylogenetic analyses conducted in this study consistently recovered a distinct yet previously unrecognized lineage that was sister to the monophyletic genus *Rossbeevera*. Morphologically, members of the two clades are readily distinguishable by differences in the basidiospores and in the sterile base of the fruiting body. The unique, minisatellite-like insertions within ITS2 nuc-rDNA were highly divergent between the two clades as well as between the different species-level lineages (Fig. 6). Based on both molecular and morphological data, we propose the new genus *Turmalinea* for this lineage. This group is comprised of three new Japanese species (*T. persicina*, *T. yuwanensis*, and *T. mesomorpha*), one subspecies (*T. mesomorpha* subsp. *sordida*) and one Chinese species (*T. chrysocarpa*). Within the genus *Rossbeevera* we propose two new species from Japan, *R. paracyanea* and *R. cryptocyanea*.

Turmalinea Orihara & N. Maek., *gen. nov.* — MycoBank MB803433

Type species. Turmalinea persicina Orihara.

Etymology. The Latinized name, *Turmalinea*, refers to tourmaline, the reddish or bluish coloured mineral, referring to the striking colour variety of the fruitbodies.

Fruitbodies mostly less than 20 mm diam, solitary to sparse, subglobose to depressed-globose to reniform, rubbery, sessile or rarely with a short stipe at the base, surface smooth to slightly felty, pale pink to pink, or white to brownish white, often turning blue to indigo-blue when rubbed or bruised. *Rhizomorphs* whit-

ish or yellow to orange. *Gleba* initially white, then maturing to blackish brown, firm, loculate, of minute irregular chambers and thin tramal plates, chambers arranged somewhat radially near centre. *Trama* mostly pulvinate, rarely becoming a short stipe, subgelatinous. *Columella* absent. *Peridium* thin, up to 450 µm in dried specimens, single- or two-layered, of interwoven to parallel, septate, filamentous hyphae. *Subhymenium* undeveloped. *Basidia* clavate to cylindrical, 2–4-spored. *Basidiospores* statismorphic, ovoid to fusoid, inamyloid, non-dextrinoid, brick-red to dark brown at maturity, with 5–10 longitudinal, often branched, costal to irregularly broken ridges up to 3.5 µm high, with or without a hilar appendage. *Clamp connections* absent in all tissues.

Notes — *Turmalinea* is morphologically characterized by ovoid to fusoid, reddish brown to dark brown basidiospores with 5–10 irregularly furcate, longitudinal ridges, and a cushion-like, subgelatinous sterile base. Two of the four species of *Turmalinea* have pinkish fruitbodies with yellow to orange rhizomorphs, which are unusual in hypogeous sequestrate fungi (Fig. 7a–d). The sister genus, *Rossbeevera* is morphologically different from *Turmalinea* in having a sterile base that often forms a short, reduced stipe and paler ellipsoid or fusoid to fusiform basidiospores that have 3–5 longitudinal ridges. *Turmalinea* also tends to form firm, depressed-globose to reniform basidiomata, which are less common in *Rossbeevera* (Fig. 7). In addition, there is a considerable genetic divergence within the ITS2 minisatellite-like insertion between the two genera, although the insertions are found at the same position in the ITS2 region (Fig. 6).

Ecologically, species of *Turmalinea* occur in broad-leaved forests and are presumably symbiotic ectomycorrhizal associates of trees in the *Fagaceae*. Although we have not confirmed their ectomycorrhizal status, it is likely that they are mycorrhizal based on the fact that most species in *Boletaceae* form ectomycorrhizas (Nuhn et al. 2013). While species of *Rossbeevera* exhibit tropical to temperate distribution and often fruit in summer, *Turmalinea* species have not yet been found in the tropics and they generally fruit during cooler weather. This might reflect physiological difference in hyphal growth between members of the two genera and, thus, might result in their distributional difference.

Another similar leccinoid sequestrate genus, *Chamonixia*, also has basidiospores with 6–12 longitudinal ridges, but the basidiospores are generally ellipsoid to broadly ellipsoid ($Q = 1.3–1.8$). Macroscopically, *Chamonixia* spp. form light, fragile fruitbodies whereas those in the *Rossbeevera-Turmalinea* lineage have a more rubbery texture. In addition, the sterile base of *Chamonixia* fruitbodies is never gelatinized, and often forms a percurrent or branched columella. The genus *Rhodactina* is a sequestrate member of *Boletaceae* reported from India and Thailand (Pegler & Young 1989, Yang et al. 2006). The genus is similar to *Turmalinea* in that the fruitbodies stain reddish to purplish and the basidiospores have 5–10 longitudinal ridges (Fig. 9k, l), but is distinctive from *Turmalinea* in the violet brown to purplish carmine gleba and well-developed (3–5 µm high), unbranched, acute ridges of the basidiospores (Yang et al. 2006; T. Orihara pers. obs.). The *ATP6* sequence from *Rhodactina incarnata* is c. 93–94 % similar to *ATP6* sequences of *Turmalinea* spp., suggesting that they are not members of the same lineage. We obtained an ITS1 sequence of the isotype of *R. incarnata* (GenBank KC552020), and the BLAST search suggests that it is most closely related to species of *Tylophilus*. The southern hemisphere genus, *Austrogautieria*, also has similar basidiospores with eight or more irregularly branched, longitudinal ridges. However, molecular phylogenetic analysis shows that *Austrogautieria* is a member of *Gallaceaceae* in the Hysterangiales (Hosaka et al. 2006), and therefore, is phylo-



Fig. 7 Fruitbodies of *Turmalinea* and *Rossbeevera* species. a. *Turmalinea persicina* (holotype); b. *Turmalinea yuwanensis* (holotype); c. aberrant fruitbody of *T. persicina* with a short stipe and incomplete lamellae (arrow) (KPM-NC 18008); d. *Turmalinea chrysocarpa* (holotype); e. *Turmalinea mesomorpha* subsp. *mesomorpha* (holotype); f. *Turmalinea mesomorpha* subsp. *sordida* (holotype); g. *Rossbeevera paracyanea* (holotype); h. *Rossbeevera cryptocyanea* (holotype). — Scale bars = 1 cm.

genetically distant from *Turmalinea*. Morphologically, species of *Austrogautieria* are readily distinguished from *Turmalinea* by the glutinous spore mass and the presence of a well-developed columella in the gleba.

***Turmalinea persicina* Orihara, sp. nov.** — MycoBank MB803437; Fig. 7a, c, 8a–e

Holotype. JAPAN, Kyoto Pref., Sakyo-ku, Iwakura-agura-cho, Mt Amabuki, c. 200 m northwest from Jisso-in Temple, under *Castanopsis sieboldii*, 8 Dec. 2008, T. Orihara, *Orihara952* (KPM-NC 18001; isotype TNS-F-55010).

Etymology. Latin, *persicina* (= peach-coloured), refers to the characteristic colour of the fruitbodies.

Fruitbodies up to 20 mm, subglobose to depressed-globose to reniform, rubbery, sessile or rarely with a reduced stipe at the base, surface covered with thin, smooth, pink to pinkish white peridium occasionally turning weakly blue to bluish green when bruised, becoming blackish pink at maturity due to blackish colour of the inner gleba. **Gleba** off-white, occasionally turning bluish green in youth when cut, then blackish brown at maturity, rubbery, composed of minute, irregular locules. **Sterile base** present, mostly pulvinate or rarely becoming a short, reduced stipe, translucent, subgelatinous. **Rhizomorphs** orange-yellow, common. **Odour** somewhat sweet but unpleasant. **Basidiospores** 13.1–20.2(–20.6) × (7.7–)7.8–10.4(–10.7) µm, mean 16.7 × 9.1 µm (SD: 1.74 (length), 0.64 (width)), Q = 1.37–2.37, $Q_m = 1.84$, symmetric, ovoid to fusoid, colourless at first then becoming dark brown at maturity, with 6–10 irregularly longitudinal, partially branched ridges up to 2.9 µm high in water, often containing one large oil drop inside, often with a distinct hilar appendage up to 4.5 µm long, $HA/S = 0.09–0.25$, $HA/S_m = 0.17$ (n = 35), spore walls 0.6–1.3 µm thick. **Basidia** evanescent, cylindrical, 17.5–30.3 × 6–8.2 µm, mean 24 × 7.3 µm (n = 10), colourless to fulvous, 2-spored, walls thin (< 0.8 µm thick), inner matrix somewhat granulate. **Basidioles** persistent, 10–40 µm diam, clavulate to subspherical, colourless, thin-walled (< 0.7 µm thick). **Trama** colourless, of compactly interwoven, sinuate, thin-walled (< 0.6 µm thick) filamentous hyphae 2.3–9 µm broad. **Sterile base** of interwoven, partially branched, sinuate, colourless to pale yellowish brown, septate, thin-walled (< 0.8 µm thick) filamentous hyphae 3–13.5 µm broad. **Peridium** 40–325 µm thick, stramineous to yellow-brown under light microscopy, composed of non-inflated, partially branched, septate filamentous hyphae 2.5–9.5 µm broad parallel to subparallel to surface forming a cutis, walls 0.5–1.5 µm thick. **Rhizomorphs** 50–100 µm broad, of a bundle of yellow-brown, straight, thin-walled (< 0.8 µm thick) filamentous hyphae, mostly 2–6 µm broad but sometimes inflated to 12 µm broad.

Habitat, Distribution & Season — Hypogeous under evergreen plants of the *Fagaceae*: *Castanopsis sieboldii*, *C. cuspidata*, and *Quercus glauca*; Japan (western Honshu, Shikoku, Kyushu); late autumn to spring (November to April), occasionally early summer (June).

Specimens examined. JAPAN, **Ehime Pref.**, Kihoku-cho, Narukawa Gorge, in the *Castanopsis* and *Quercus* forest, 25 Oct. 2010, F. Nagao, *Nagao 10-10-25-02*, KPM-NC 17744; **Kyoto Pref.**, Kyoto-shi, Higashiyama-ku, Mt Kiyomizu, near Shogun-zuka, under *Castanopsis cuspidata*, 28 Nov. 2004, A. Kajiyama, *Orihara225*, KPM-NC 17851; same locality, 20 Nov. 2005, T. Orihara, *Orihara354*, KPM-NC 17857; same locality, 26 Nov. 2006, T. Orihara, *Orihara555*, KPM-NC 17853; same locality, 27 Apr. 2008, T. Orihara, *Orihara775*, KPM-NC 17854; same locality, parasitized by *Sepedonium chrysospermum*, 27 Apr. 2008, T. Orihara, *Orihara775b*, KPM-NC 17857; same locality, 22 Feb. 2009, T. Orihara, *Orihara955*, KPM-NC 17858; Kyoto-shi, Sakyo-ku, Iwakura-agura-cho, Mt Amabuki, under *Castanopsis sieboldii*, 7 Nov. 2005, Y. Kotera & T. Orihara, *Orihara339*, KPM-NC 17852; same locality, 8 Dec. 2008, T. Orihara, *Orihara952* (holotype KPM-NC 18001; isotype TNS-F-55010); same locality, 10 Dec. 2011, T. Orihara & Y. Kotera, KPM-NC 18009; **Mie Pref.**, Seki-machi, near Shoho-ji Temple, under *C. sieboldii*, 2 June 2008, M. Ohkubo & T. Orihara, *Orihara776*, KPM-NC 17856;

Hyogo Pref., Shiogahara, under *C. cuspidata*, 20 Nov. 2011, M. Ohmae, KPM-NC 18053; **Hiroshima Pref.**, Hiroshima-shi, Higashi-kum Hukuda-cho, under *Q. glauca*, 23 Oct. 2010, A. Hadano, *Orihara1291*, KPM-NC 18002; same locality, parasitized by *S. chrysospermum*, 23 Oct. 2010, A. Hadano, *Orihara1292*, KPM-NC 18003; **Nara Pref.**, Nara-shi, Mt Kasuga Primeval Forest, under *C. sieboldii*, 3 Nov. 2010, T. Orihara, *Orihara1345*, KPM-NC 18004; same locality, 11 Dec. 2012, H. Inui, M. Inui & T. Orihara, KPM-NC 18056; same locality, 12 Dec. 2012, H. Inui, M. Inui & T. Orihara, KPM-NC 18057 (duplicate TNS-F-55012); same locality, 12 Dec. 2012, H. Inui, M. Inui & T. Orihara, KPM-NC 18058; **Oita Pref.**, Saiki-shi, Shiroyama Park, under *C. sieboldii*, 15 Jan. 2011, Y. Sunada & T. Orihara, *Orihara1363*, KPM-NC 18006; Saiki-shi, Nakayama, near Shirohachiman Shrine, under *C. sieboldii*, 15 Jan. 2011, Y. Sunada & T. Orihara, *Orihara1364*, KPM-NC 18007 (duplicate: TNS-F-55011); Saiki-shi, Ume-oaza, Shigeoka, 1.5 km southwest from Sotaro Station, under *C. sieboldii*, 16 Jan. 2011, Y. Sunada & T. Orihara, *Orihara1368*, KPM-NC 18008; **Yamaguchi Pref.**, Yamaguchi-shi, Tokuchi, near the Lake Ohara, under *C. cuspidata* and *Q. serrata*, 28 Nov. 2014, Y. Kawaguchi, KPM-NC 23395.

Notes — *Turmalinea persicina*, which is widely distributed throughout western Japan, is easily distinguished from other species by its pinkish white to pale pink fruitbodies with yellow to orange rhizomorphs at the base. The large, persistent, inflated basidioles are also characteristic of the species (Fig. 8b). Like other species of *Turmalinea*, its sterile base is mostly pulvinate, but we found one fruitbody with a distinct stipe and a trace of hymenophoral pores (Fig. 7c; KPM-NC 18008). However, DNA sequences from this specimen were nearly identical to other, more typical specimens collected nearby (i.e., KPM-NC 18007 and KPM-NC 18008). This is an example of the high morphological plasticity of sequestrate fungi, sometimes caused by only a few nucleotide substitutions in key functional genes, which might be expected during the evolution of sequestrate taxa from epigeous relatives (Thiers 1984, Bruns et al. 1989, Kendrick 1992, Bougher et al. 1993, Hibbett et al. 1994).

***Turmalinea yuwanensis* Orihara, sp. nov.** — MycoBank MB803438; Fig. 7b, 8f–j

= *Hymenogaster* sp., in Yoshimi & Doi, Mem. Natl. Sci. Mus. (Tokyo) 22: 36. 1989.

Holotype. JAPAN, Kagoshima Pref., Amami-oshima Island, Yamato-son, southeast foot of Mt Yuwan, 29 Nov. 2008, T. Orihara, A. Okuda, M. Ohmae, *Orihara942*, KPM-NC 18011.

Etymology. The epithet, *yuwanensis*, refers to the type locality of the species, Mt Yuwan-dake, which is located in Amami-oshima Island, Kagoshima Pref., Japan.

Fruitbodies up to 20 mm, depressed-globose to reniform, rubbery, sessile or a short, rudimentary stipe at the base, peridium surface smooth, vivid pink but white to pinkish white near the base, colour change not observed when rubbed or bruised, becoming dull pink at maturity due to a blackish colour of the inner gleba. **Gleba** white in youth, then blackish brown at maturity, rubbery, composed of minute, irregular locules. **Sterile base** present, mostly pulvinate, translucent, subgelatinous, colourless when immature then becoming dull yellowish brown. **Rhizomorphs** vivid yellow, often developed. **Odour** somewhat sweet but unpleasant, similar to that of *Turmalinea persicina*. **Basidiospores** 11.2–(11.4–)14.6(–14.5) × 7–(7.1–)8.8(–9) µm, mean 12.9 × 7.9 µm (SD: 0.86 (length), 0.44 (width)), Q = 1.41–1.84, $Q_m = 1.64$, ovoid to citriform to fusoid, colourless at first then becoming dark brown at maturity, with 5–10 irregularly longitudinal ridges 1.5–3.5 µm high and 2–4.1 µm wide in water, but the ridges mostly broken, becoming somewhat flat, large warts, a hilar appendage often present but relatively undeveloped, usually less than 3 µm long, $HA/S = 0.09–0.24$, $HA/S_m = 0.16$ (n = 20), occasionally with a hyaline pedicel up to 5.5 µm long, spore walls 0.7–1.2 µm thick. **Basidia** evanescent, cylindro-clavate, 16.7–32.2 × 6.8–9 µm, mean 24.8 × 8.1 µm (n = 10), colourless, 2–4-spored, walls thin (< 0.8 µm thick),

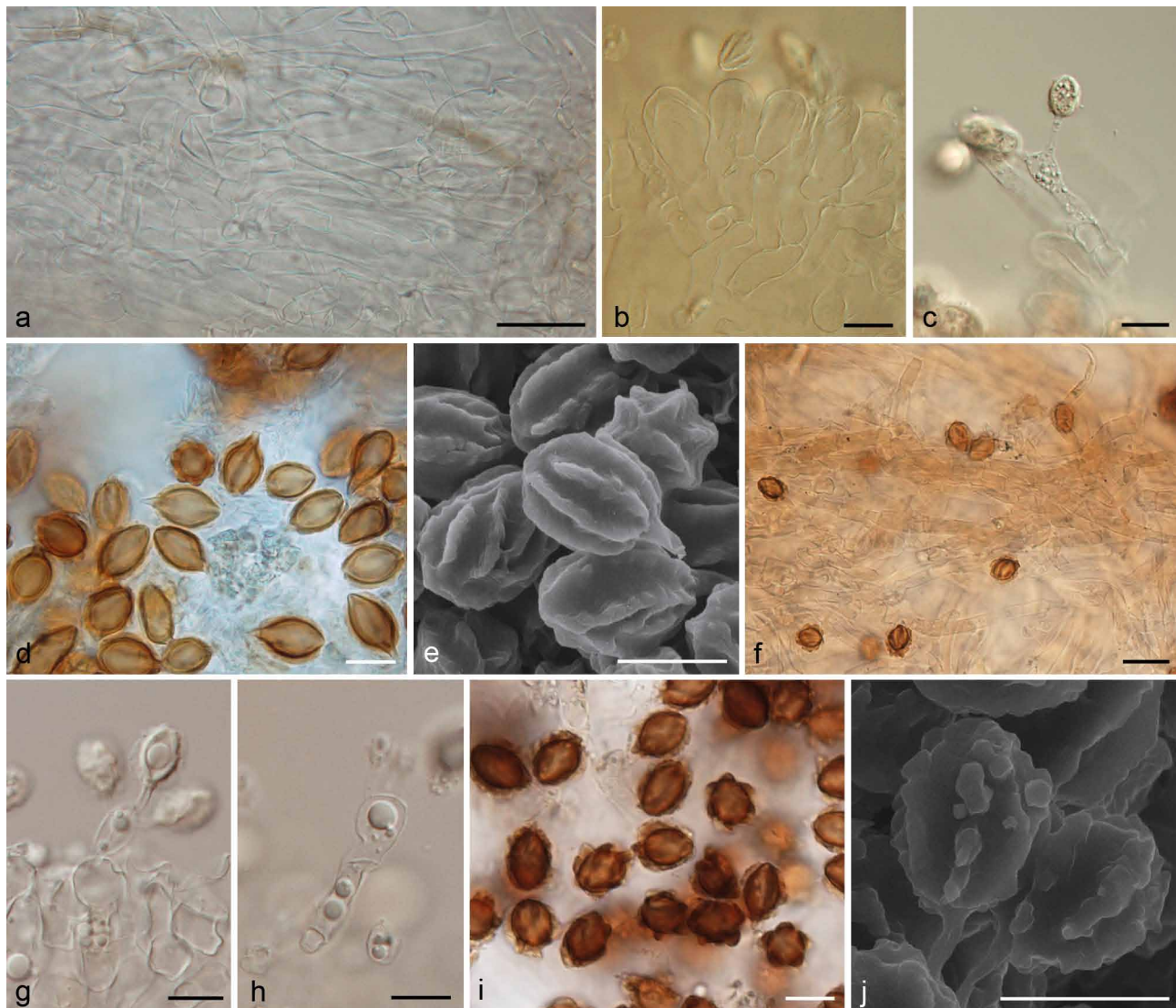


Fig. 8 a–e: *Turmalinea persicina*. a. Peridial hyphae (KPM-NC 17744); b. hymenium with inflated basidioles (KPM-NC 17744); c. 2-spored basidium (KPM-NC 18001, holotype); d. basidiospores (KPM-NC 18007); e. SEM image of basidiospores (holotype). — f–j: *Turmalinea yuwanensis* (holotype): Peridial hyphae; g–h. 3- and 4-spored basidia; i. basidiospores; j. SEM image of basidiospores. — Scale bars: a, f = 20 μ m; b–e, g–j = 10 μ m.

inner matrix inconspicuous, contains several oil drops, sterigmata 4.5–7 μ m long. *Basidioles* persistent, 8–20 μ m diam, clavulate to subspherical to vesiculate, colourless, thin-walled (< 0.8 μ m thick). *Trama* white colourless, of compactly interwoven, thin-walled (< 0.8 μ m thick) filamentous hyphae 2–9 μ m broad. *Sterile base* of compactly interwoven, thin-walled (< 0.8 μ m broad), colourless to pale yellowish brown, septate filamentous hyphae 3–10.5 μ m broad. *Peridium* 150–400 μ m thick, in the outer part stramineous to yellow-brown under light microscopy, in the inner part almost colourless, composed of interwoven to subparallel, partially branched, non-inflated, septate filamentous hyphae 3–10(–13.5) μ m broad forming a cutis, walls up to 1 μ m thick.

Habitat, Distribution & Season — Hypogeous to subepigeous under or on rotten wood of *Castanopsis sieboldii* subsp. *lutchuensis*; So far known from Amami-oshima, Okinawa and Tokashiki Islands, the Ryukyu Archipelago, Japan; late autumn (November).

Specimens examined. JAPAN, **Kagoshima Pref.**, Amami-oshima Island, Naze-shi, Kinsakubaru National Forests, 19 Nov. 1988, Y. Doi, '*Hymenogaster* sp.', *Yoshimi7393*, TNS-F-183213; Amami-oshima Island, Yamato-son, southeast foot of Mt Yuwan, under *Castanopsis sieboldii* subsp. *lutchuensis*, 17 Nov. 2007, A. Hadano, T. Orihara, M. Ohkubo, *Orihara758*, KPM-NC 18010 (duplicate: TNS-F-55013); same locality, 29 Nov. 2008, T. Orihara, A. Okuda, M. Ohmae, *Orihara942*, KPM-NC 18011 (holotype); **Okinawa Pref.**, Tokashiki-jima Island, Tokashik-son, Tokashiki, under *Castanopsis sieboldii*

subsp. *lutchuensis*, 14 Apr. 2013, T. Orihara, KPM-NC 23377; Okinawa Island, Kunigami-son, along the path to Mt Yonaha, under *Castanopsis sieboldii* subsp. *lutchuensis*, 10 Nov. 2013, M. Moriguchi, KPM-NC 23390; same locality, 5 Feb. 2015, T. Orihara, KPM-NC 23998; same locality, 5 Feb. 2015, T. Orihara, KPM-NC 24000.

Notes — The vivid pink peridial surface and yellow rhizomorphs of *Turmalinea yuwanensis* are striking features and are easily recognized in the field. Microscopically, *T. yuwanensis* is unique in that its basidiospores have distinct but discontinuous longitudinal ridges that partially become large, irregular warts. A similar and closely related species, *T. persicina*, is distinguished from *T. yuwanensis* by the paler peridium, larger basidiospores with relatively continuous ridges, and its slender, 2-spored basidia. The Chinese species, *T. chrysocharpa* is also phylogenetically close to *T. yuwanensis*, but is readily distinguished by the yellow peridium and larger basidiospores (Fig. 8d).

This species has been collected from only a few sites in the central Ryukyu Islands, which lie c. 300–600 km to the southwest of mainland Japan. A truffle-like fruitbody with orange rhizomorphs reported by Yoshimi & Doi (1989) from Amami-oshima island as '*Hymenogaster* sp.' was confirmed as an immature *T. yuwanensis*. Given the unique phylogenetic position and rarity of *T. yuwanensis*, the conservation of its habitat is of primary importance in terms of phylogenetic diversity (Faith 1992, Faith & Baker 2006).

Turmalinea chrysocarpa Orihara & Z.W. Ge, *sp. nov.* — MycoBank MB803441; Fig. 7d, 9a–c

Holotype. CHINA, Yunnan Prov., Manhao, Gejiu, alt. 860 m, in a broad-leaved forest, 24 Sept. 2011, Z.W. Ge 3098 (HKAS70601; isotype KPM-NC 18068).

Etymology. The Latin, *chryso-* (golden) and *-carpa* (fruitbody), refer to the colour of the fruitbody surface of the species, which is unusual in *Turmalinea*.

Fruitbody solitary, 1.5 cm diam, depressed-globose, surface smooth to slightly floccose, yellow to light orange, stipe reduced, rudimentary, with orange rhizomorphs at the base. *Gleba* chocolate brown to blackish brown at maturity, composed of minute, irregular locules. *Sterile base* present, more or less pulvinate, translucent, subgelatinous. *Odour* strong and sweet. *Basidiospores* 13.5–(13.8–)21.5(–23.5) × (6.9–)7.3–9.7(–10.8) µm, mean 17.5 × 8.5 µm (SD: 1.97 (length), 0.61 (width)), $Q = 1.66–2.71$, $Q_m = 2.06$, symmetric, citriform to fusiform, dark reddish brown at maturity, with 6–9 irregularly longitudinal, often furcate ridges 1–2.2 µm high in water, with a distinct hilar appendage up to 6 µm long, $HA/S = 0.11–0.31$, $HA/S_m = 0.19$, spore walls 0.7–1.2 µm thick. *Basidia* evanescent, cylindrical but mostly collapsed, 20.9 × 3.2 µm, 2-spored, colourless, sterigmata up to 7.5 µm long. *Trama* colourless, of moderately or somewhat loosely interwoven, partially sinuate, septate filamentous hyphae 2–10 µm broad, walls up to 1.2 µm thick. *Peridium* 150–330 µm thick, composed of two layers: outermost layer (i.e., peridiopellis) 60–150 µm thick, of parallel to subparallel, straight, septate, colourless, thin-walled (< 0.8 µm), non-inflated filamentous hyphae 2.8–10(–13) µm broad, only the surface stained fulvous; inner layer (i.e., subpellis) 75–250 µm thick, colourless, of compactly interwoven, sinuate, septate, narrower (2.5–8 µm), thin-walled filamentous hyphae.

Notes — *Turmalinea chrysocarpa*, which is reported from Southwest China, is unique in having a yellow to light orange peridium and an inner peridial layer composed of compact, interwoven hyphae. Phylogenetic analyses support that *T. chrysocarpa* is a distinct lineage from the other *Turmalinea* spp. from Japan (Fig. 3–6). This species is readily distinguished from other members of the genus by the colour of the peridium and the dimension of basidiospores. Unfortunately, only one specimen of *T. chrysocarpa* has so far been collected. Although this may be due to the rarity of the species, it may also be due to lack of data on the diversity, phenology and ecological requirements of sequestrate fungi in China. Despite our lack of knowledge about this species, its characteristic morphology and phylogenetic distinctness are sufficient to describe it as a new *Turmalinea* species.

Turmalinea mesomorpha Orihara, *sp. nov.* — MycoBank MB803439; Fig. 7e, 9d–g

Holotype. JAPAN, Aomori Pref., Towada-shi, Ohoronai, under *Fagus crenata*, 12 Oct. 2009, T. Sasa & T. Orihara, *Orihara1080*, KPM-NC 18015.

Etymology. The Latin, *meso-* (middle or intermediate) and *-morpha* (morphology), signifying that the species has intermediate morphology between *Rossbeevera* spp. and other members of *Turmalinea*.

Subspecies autonym. *Turmalinea mesomorpha* subsp. *mesomorpha* (the automatically generated name by the proposal of *T. mesomorpha* subsp. *sordida*, which is to be described below).

Fruitbodies up to 24 mm, subglobose to depressed-globose to reniform, rubbery, sessile or with a short, reduced stipe less than 5 mm long at the base, surface somewhat felty or partially wrinkled, white to off-white, immediately turning indigo to purplish blue and finally blackish brown when touched or bruised. *Gleba* off-white to whitish yellow when immature, then chocolate brown, and finally becoming blackish brown at maturity, rubbery, composed of minute, irregular locules. *Sterile base* present,

mostly pulvinate but rarely columella-like, translucent, subgelatinous, colourless to blue-grey when immature then becoming dull yellowish brown at maturity, surrounded by whitish hyphal veins irregularly radiating from the central sterile base and connected to inner portion of the peridial context at the bottom. *Rhizomorphs* white to off-white, common, showing the same pattern of discolouration as the fruitbody surface. *Odour* somewhat sweet but unpleasant. *Basidiospores* 12.5–16.4(–16.9) × (7.8–)7.9–10.4 µm, mean 14.4 × 9.1 µm (SD: 0.97 (length), 0.61 (width)), $Q = 1.38–1.92$, $Q_m = 1.58$, symmetric, ovoid to citriform to fusoid, colourless at first then becoming dark reddish brown at maturity, with 5–10 irregularly longitudinal, costal or often branched ridges up to 2.6 µm high in water, a hilar appendage reduced or indistinct, occasionally with a hyaline pedicel up to 6 µm long, spore walls 0.7–1.6 µm thick. *Basidia* evanescent, clavate to cylindro-clavate, 25.5–43.8 × 6.4–12.2 µm, mean 33.1 × 8.8 µm ($n = 15$), 2–4-spored, colourless or with a yellowish brown tint, sterigmata 6–10.5 µm long, walls thin (< 0.8 µm thick), inner matrix somewhat granulate. *Basidioles* cylindrical to cylindro-clavate, 10–18 × 6–9 µm, colourless or pigmented fulvous, walls thin (< 0.7 µm thick). *Trama* colourless or pigmented pale yellowish brown in places, of subparallel to loosely interwoven, straight, partially branched, thin-walled (< 0.8 µm thick) filamentous hyphae 2–10 µm broad. *Sterile base* of loosely interwoven, mostly sinuous, colourless, septate, thin-walled (> 0.8 µm thick) filamentous hyphae 3.5–11 µm broad, the surrounding whitish layer composed of loosely interwoven, more or less frequently branched, thin-walled (< 0.8 µm thick), filamentous hyphae 2–8 µm broad that are less sinuate than those comprising the sterile base. *Peridium* 50–150 µm thick, yellow-brown under light microscopy, composed of repent, partially branched and inflated, septate filamentous hyphae 2–11 µm broad interwoven or subparallel to surface, walls up to 1 µm thick.

Habitat, Distribution & Season — Hypogeous to subepigeous under *Fagus crenata*; Japan (northern Honshu); autumn (September to October).

Specimens examined. JAPAN, **Aomori Pref.**, Towada-shi, Ohoronai, under *Fagus crenata* (the holotype locality), 21 Sept. 2008, T. Sasa, *Orihara874*, KPM-NC 18012 (duplicate: TNS-F-55014); same locality, 12 Oct. 2009, T. Sasa & T. Orihara, *Orihara1080*, KPM-NC 18015 (holotype); Towada-shi, Tsutaonsen, under *F. crenata*, 27 July 2012, T. Muroi, KPM-NC 18059; **Iwate Pref.**, Hachimantai-shi, Appi-kohgen, under *F. crenata*, 11 Oct. 2009, M. Taniguchi, *Orihara1074*, KPM-NC 18013; same locality, 12 Oct. 2009, T. Sasa & T. Orihara, *Orihara1075*, KPM-NC 18014.

Notes — *Turmalinea mesomorpha*, the earliest diverging species within *Turmalinea*, shares characteristics of both *Turmalinea* and *Rossbeevera*. Like most *Rossbeevera* species, the fruitbody has a whitish peridium that quickly turns indigo to purplish blue. On the other hand, most other generic level characters such as the cushion-like sterile base and the basidiospore morphology are typical of *Turmalinea*. The morphology of *T. mesomorpha* in combination with its position in the phylogeny suggests that the pinkish to yellow colours of the other *Turmalinea* species probably evolved after the divergence of *T. mesomorpha*. Compared to other *Turmalinea* species, the sterile base tends to become amorphous and surrounded with whitish hyphal veins. Interestingly, one fruitbody (KPM-NC 18059) had a columnar sterile base, which is more common in *Rossbeevera*. These peridial and sterile base characters morphologically support that the species is the earliest diverging lineage within the genus *Turmalinea*. Moreover, the aberrant sterile base morphologies found in *T. mesomorpha* and *T. persicina* suggest that these reversions have occurred somewhat frequently within the genus.

Turmalinea mesomorpha is microscopically different from *T. persicina* and *T. yuwanensis* in its larger basidia and medium-sized

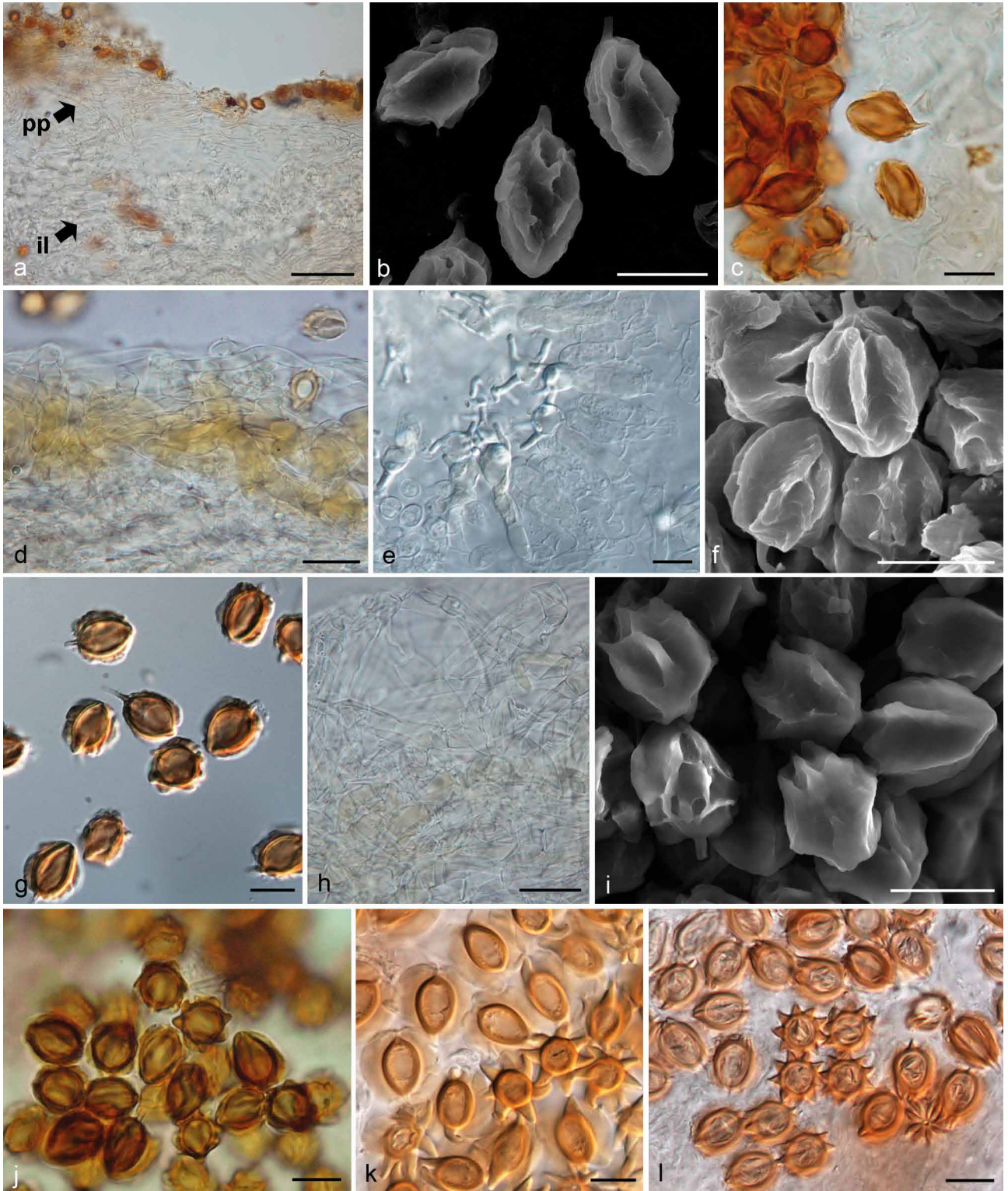


Fig. 9 a–c: *Turmalinea chrysocarpa* (HKAS 70601, holotype). a. Peridium (arrows: pp = outer layer (peridiopellis); il = inner layer); b. SEM image of basidiospores; c. basidiospores. — d–g: *Turmalinea mesomorpha* subsp. *mesomorpha*. d. Peridial hyphae (KPM-NC 18014); e. basidia (KPM-NC 18014); f. SEM image of basidiospores (KPM-NC 18015, holotype); g. basidiospores (holotype). — h–j: *Turmalinea mesomorpha* subsp. *sordida*. h. Peridial hyphae (KPM-NC 17743); i. SEM image of basidiospores (KPM-NC 18016, holotype); j. basidiospores (holotype). — k–l: Basidiospores of *Rhodactina* spp. k. *Rhodactina himalayensis*; l. *Rhodactina incarnata*. — Scale bars: a = 50 μ m; b, c, e–g, i–l = 10 μ m; d, h = 20 μ m.

basidiospores with relatively continuous longitudinal ridges. In contrast to *T. persicina* and *T. yuwanensis*, which occur in the evergreen *Quercus/Castanopsis* forest, *T. mesomorpha* has only been collected under the deciduous montane tree *Fagus crenata*. This suggests not only geographical but also ecological isolation from the other two Japanese *Turmalinea* species.

***Turmalinea mesomorpha* subsp. *sordida* Orihara, subsp. nov.** — MycoBank MB803440; Fig. 7f, 9h–j

Holotype. JAPAN, Ehime Pref., Saijo-shi, Mt Ishizuchi, under *F. crenata*, 10 Oct. 2010, H. Ikeda, Orihara1280, KPM-NC 18016.

Etymology. The Latin, *sordida* (= dirty, foul), refers to the characteristic colour of the peridial surface of the subspecies.

Diagnosis. This subspecies is distinguished from *Turmalinea mesomorpha* subsp. *mesomorpha* by the greyish brown surface of fruitbodies that

turns deep blue to purple and finally becoming blackish brown when touched or bruised, and thicker peridium up to 450 µm thick composed of filamentous hyphae 3–15 µm broad. *Basidiospores* shape and dimensions not significantly different from that of *T. mesomorpha* subsp. *mesomorpha*, 11.7–(12–)15.6(–17) × (6.8–)7.3–9.6 µm, mean 13.7 × 8.5 µm (SD: 0.96 (length), 0.58 (width)), $Q = 1.41–1.94$, $Q_m = 1.62$.

Habitat, Distribution & Season — Hypogeous to subepigeous under *Fagus crenata*; Japan (Shikoku); autumn (September to October).

Specimens examined. JAPAN, **Ehime Pref.**, Saijo-shi, Mt Ishizuchi, under *F. crenata*, 10 Oct. 2010, H. Ikeda, Orihara1280, KPM-NC 18016 (holotype); Matsuyama-shi, Mt Takanawa, under *F. crenata*, 4 Nov. 2007, F. Nagao, KPM-NC 17743.

Notes — The *T. mesomorpha* specimens collected from Shikoku, one of the four main islands of Japan, showed slight macroscopic differences from the other collections from the northern part of Japan, including the holotype specimen of subsp. *mesomorpha*. However, we did not find any significant microscopic differences between the two groups, and they share a similar ecological habitat (i.e., they are all found in association with Japanese beeches). The phylogenetic analyses conducted in this study showed slight divergence between the two lineages, suggesting their relatively recent diversification compared to the other species-level lineages in the genus. We therefore recognize the Shikoku lineage as subspecies *sordida* based on morphological and molecular data that are currently available.

Aoki (1978) informally reported a specimen from Tokyo that more or less fit the characters of *T. mesomorpha* subsp. *sordida* as '*Gautieria* sp.'. However, we were unable to locate this specimen, so we could not directly compare it to our recently collected material. Since Tokyo is geographically intermediate between the present habitats of each subspecies, the record or additional collections in that area should provide important knowledge about the biogeography of the species in the future.

Rossbeevera T. Lebel & Orihara, in Lebel et al., *Fung. Diversity* 52: 54 + 73. 2012, '*Rosbeeva*'.

Type species. *Rossbeevera pachydermis* T. Lebel, *Fung. Diversity* 52: 64. 2012, '*Rosbeeva pachyderma*'.

Notes — The precise description of *Rossbeevera* is presented in Lebel et al. (2012a) under the variant '*Rosbeeva*'. Since the correction of the type species name is omitted in the erratum by Lebel et al. (2012b), we herein specify its correct name.

Rossbeevera paracyanea Orihara, *sp. nov.* — MycoBank MB803442; Fig. 7g, 10a–e

Holotype. JAPAN, Nara Pref., Nara-shi, Nara Park, under *Quercus gilva*, 26 Oct. 2008, M. Kawai, Orihara908, KPM-NC 17847.

Etymology. The epithet (Greek, *para-* = para- or beside and *cyanea* = ultramarine blue) expressing the morphological characteristics, habitat and distribution of the species similar to those of *Rossbeevera eucyanea*: both of the species have strongly cyanescent fruitbodies and occur usually under *Castanopsis* and evergreen *Quercus* trees in western Japan.

Fruitbodies solitary or in small clusters, up to 27 mm diam, subglobose to depressed-globose, soft, peridial surface smooth, white to greyish at first, becoming dark blue-grey to dark grey and occasionally cracked at maturity to expose inner gleba and turning deep blue when touched or bruised. *Gleba* off-white when immature, dark reddish brown at maturity, non-gelatinous, minutely and irregularly loculate, turning indigo-blue in some portions when cut and exposed to air. *Sterile base* present but reduced, non-gelatinous, strongly cyanescent, often forming

a short stipe. *Columella* absent. *Odour* somewhat sweet but unpleasant. *Basidiospores* (13.3–)14–19.3(–20.4) × (6.7–)6.9–9.2(–9.3) µm, mean 16.7 × 8 µm (SD: 1.32 (length), 0.57 (width)), $Q = 1.7–2.5$, $Q_m = 2.1$, symmetric, fusoid to fusiform, inamyloid, nondextrinoid, colourless at first then becoming reddish brown at maturity, with 4–5 or rarely 3 smooth, longitudinal ridges up to 2.5 µm high in water, walls 0.5–1.2 µm thick, with a developed hilar appendage 2.1–4.5(–4.7) µm long (mean 3.3 µm) at the base, $HA/S = 0.13–0.25$, $HA/S_m = 0.2$, walls at the tips thinner than on the sides. *Basidia* 13.8–21 × 6–11 µm (mean = 18 × 8.1 µm; n = 10), clavulate to doliform, evanescent, colourless or pigmented with yellow-brown, mostly 2-spored but rarely 1-, 3- or 4-spored. *Hymenium* developed when immature but collapsed at maturity, colourless; *basidioles* clavate to clavulate to doliform almost the same size as or smaller than basidia. *Subhymenium* not developed, composed of single- or two-layered, colourless, isodiametric to clavulate cells 4–15 µm diam. *Trama* of parallel to subparallel, non-inflated, colourless, thin-walled (< 0.6 µm thick) filamentous hyphae 2.5–5.5 µm broad. *Sterile base* composed of compact, interwoven, septate, inflated, thin-walled (c. 1 µm thick) filamentous hyphae 2–18 µm broad. *Peridium* thin, composed of 2 layers: outer layer 50–160 µm thick, of compact, interwoven, septate, pale brown to brown filamentous hyphae 2–9.5 µm swollen in some portion to 15 µm broad, walls up to 1.2 µm thick; inner layer 15–55 µm thick, tan to reddish brown, of subparallel or tangled, sinuate, non-inflated filamentous hyphae 1.5–5 µm broad, walls 0.5–1.3 µm thick. *Clamp connections* absent in all tissues.

Habitat, Distribution & Season — Hypogeous to subepigeous under *Quercus gilva* and *Castanopsis cuspidata*; Japan (western Honshu); summer to early winter (July to December).

Specimens examined. JAPAN, **Nara Pref.**, Nara-shi, Nara Park, under *Quercus gilva*, 26 Oct. 2008, M. Kawai, Orihara908, KPM-NC 17847 (holotype); Nara-shi, Mt Kasuga Primeval Forest, under *Quercus gilva*, 24 Dec. 2011, T. Orihara, KPM-NC 18022; same locality and date, T. Orihara, KPM-NC 18023; same locality, 12 Dec. 2012, T. Orihara, H. Inui, M. Inui, KPM-NC 18087; same locality, 16 Nov. 2013, M. Ohmae, KPM-NC 23940; same locality, 19 July 2014, M. Ohmae, KPM-NC 23953; same locality and date, M. Ohmae, KPM-NC 23954; **Osaka Pref.**, Minoh-shi, Mt Minoh, 5 July 2010, M. Ohmae, Orihara1178, KPM-NC 17848; same locality, 7 Aug. 2011, M. Ohmae, KPM-NC 18027; same locality, 21 July 2014, R. Nakano, KPM-NC 23955; same locality, 15 July 2014, M. Ohmae, KPM-NC 23956.

Notes — Fruitbodies of *Rossbeevera paracyanea* are macroscopically similar to those of another Japanese species, *R. eucyanea*, especially when young. Its habitat and size of basidiospores also overlap with those of *R. eucyanea*. However, *R. paracyanea* is morphologically distinguished from *R. eucyanea* by its two-layered peridium comprised of the outer layer of partially inflated, filamentous hyphae and the thin, inner layer of somewhat pigmented, sinuate filamentous hyphae. The peridium tends to peel off at maturity due to the fact that the hyphae of the inner peridial layer are more or less parallel to the surface of the gleba. The surface of *R. paracyanea* fruitbodies was generally greyish or blue-grey and this helps to distinguish the species from *R. eucyanea*, which has a whitish fruitbody.

The three-locus nuclear phylogeny showed distinct divergence within *R. paracyanea* (i.e., lineages 1 and 2), but the mitochondrial phylogeny showed a conflicting relationship (Fig. 5). In the *R. paracyanea* lineage 2 specimen from Osaka Pref. (KPM-NC 17848), some of the basidia have unusually long sterigmata (up to 20 µm long) and the context of the outer layer of the peridium was almost colourless. The latter observation, however, could be due to the immature state of the specimens. Thus, we leave the species as a single taxon and treat the collections from Osaka (KPM-NC 17848 and KPM-NC 18027) as an infraspecific cryptic lineage until sufficient collections become available for additional phylogenetic and morphological comparisons.

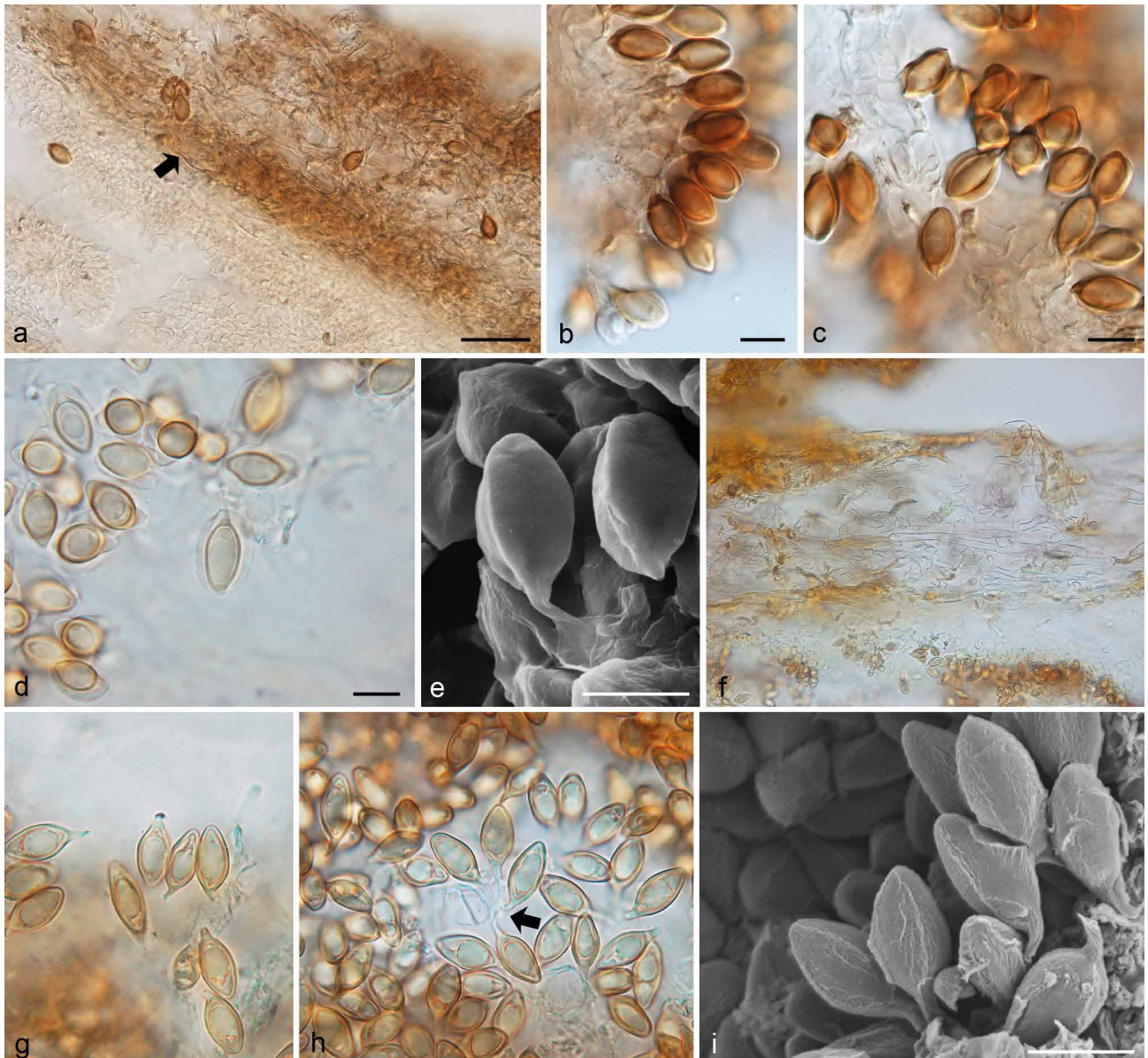


Fig. 10 a–e: *Rossbeevera paracyanea* (a–d: KPM-NC 17847, holotype; e: KPM-NC 23940). a. Peridium (upper right). The inner peridial layer is indicated by an arrow; b. basidia and basidiospores; c. mature basidiospores; d. basidiospores mounted in lacto-glycerol after pre-soaking in 3% KOH; e. SEM image of basidiospores. — f–i: *Rossbeevera cryptocyanea* (KPM-NC 23928, holotype). f. Peridium; g. basidiospores; h. basidiospores extending from a 4-spored basidium; i. SEM image of basidiospores. — Scale bars: a, f = 50 μm ; b–e, g–i = 10 μm .

***Rossbeevera cryptocyanea* Orihara** — MycoBank MB811526;
Fig. 7h, 10f–i

Holotype. JAPAN, Kakeroma Isl., Setouchi-machi, Akitoku, under *Castanopsis sieboldii* subsp. *lutchuensis*, 28 June 2014, T. Orihara, KPM-NC 23928.

Etymology. The epithet (Greek, *crypto-* = crypto- or hidden, and *cyanea* = ultramarine blue) expressing its close phylogenetic relationship and extreme morphological similarity to *R. eucyanea*.

Diagnosis. Morphologically quite similar to *Rossbeevera eucyanea*, but differs in smaller and narrower basidiospores with longer hilar appendices.

Fruitbodies solitary or in small clusters, up to 22 mm, subglobose to depressed-globose to reniform, soft, surface smooth to somewhat felty, white or more rarely greyish white, quickly turning deep blue when touched or exposed to air. *Gleba* off-white when immature, then becoming brown, non-gelatinous, minutely and irregularly loculate, quickly turning indigo-blue when cut and exposed to air. *Sterile base* present but reduced, non-gelatinous, cyanescent, forming a short stipe. *Columella* absent. *Odour* somewhat sweet but unpleasant. *Basidiospores* 13.4–(13.5–)18.3(–18.4) \times 5.8(–7.2)–7.3 μm , mean 15.8 \times 6.5 μm (SD: 1.2 (length), 0.36 (width)), $Q = 1.9$ –3.0, $Q_m = 2.4$,

fusoid to fusiform, colourless at first then becoming dark brown, with 3–5(–6) longitudinal ridges up to 2 μm high in water, walls 0.5–1.2 μm thick, with large, developed hilar appendix 2.4–5.9 μm long (mean 3.7 μm) at the base, $HA/S = 0.17$ –0.37, $HA/S_m = 0.23$. Spore walls at the tips tend to be thinner than on the sides. Basidia 12.5–21 \times 7–11.5 μm , clavate to clavate, colourless, 2- or 4-spored. Trama composed of interwoven, septate, colourless, thin-walled, filamentous hyphae 3–8 μm broad. *Peridium* 50–180 μm thick in dried specimens, of somewhat loosely woven, septate, partially branched or swollen, thin-walled (< 0.5 μm) filamentous hyphae 3–15 μm , subparallel to surface, surface often stained blue. *Clamp connections* absent in all tissues.

Habitat, Distribution & Season — Hypogeous to subepigeous under *Castanopsis sieboldii* subsp. *lutchuensis* and *Quercus glauca*; Japan (Kyushu and the Ryukyu Archipelago); early summer and late autumn (June to November).

Specimens examined. JAPAN, **Oita Pref.**, Usuki-shi, Shimonoe, under *Quercus glauca*, 20 Nov. 2005, Y. Sunada, Orihara1351, KPM-NC 17846; **Kago-shima Pref.**, Amami-oshima Isl., Yamato-son, north-eastern foot of Mt Yuwandake, under *Castanopsis sieboldii* subsp. *lutchuensis*, 17 Nov. 2007, A. Hadano & T. Orihara, Orihara760, KPM-NC 17843; Kakeroma Isl., Setouchi-

machi, Akitoku, under *Castanopsis sieboldii* subsp. *lutchuensis*, 28 June 2014; T. Orihara, KPM-NC 23928 (holotype); **Okinawa Pref.**, Ishigaki Isl., Ishigaki-shi, near Omoto tunnel, under *Castanopsis sieboldii* subsp. *lutchuensis*, 11 Oct. 2013, M. Suyama, KPM-NC 23387.

Notes — Macroscopically, *R. cryptocyanea* is indistinguishable from *R. eucyanea*: they both have white fruitbodies immediately discolouring indigo-blue to ultramarine when touched and share the same habitat in the southern part of Japan (i.e., they both occur under evergreen trees of the *Fagaceae*). The only reliable diagnostic character is the basidiospore morphology. Basidiospores of *R. cryptocyanea* are narrower than that of *R. eucyanea* ($Q = 1.9\text{--}3$ vs $1.6\text{--}2.2$; $Q_m = 2.4$ vs 1.9), and the hilar appendix of *R. cryptocyanea* basidiospores is much longer than that of *R. eucyanea*. This results in a distinct difference between their HA/S values and, hence, their basidiospore proportion: HA/S of *R. eucyanea* is significantly smaller than that of *R. cryptocyanea* (i.e., $HA/S = 0.11\text{--}0.18$, $HA/S_m = 0.14$ in *R. eucyanea*; $n = 25$).

DISCUSSION

Phylogeny, evolution, phylogeography and morphology of Rossbeevera and Turmalinea

In this study, we took several different phylogenetic approaches, including nuclear and mitochondrial multi-locus analyses, to clarify evolutionary relationships of *Rossbeevera* and the allied taxa in the leccinoid clade. The nuclear three-locus phylogeny based on the combined dataset confirmed that sequestrate fungi fall into several distinct lineages within the leccinoid clade and this phylogeny also elucidated the placement of the new generic sequestrate lineage, *Turmalinea* (Fig. 3). Loss of forcible spore discharge (i.e., ballistospory) on the process of evolution of sequestrate morphology is thought to be irreversible (Hibbett 2004, Wilson et al. 2011). The major morphological characteristics of the sequestrate genera *Chamonixia* and *Octaviania*, such as basidiospores and gleba structure, are quite different from each other and from *Rossbeevera* and *Turmalinea* (Lebel et al. 2012a, Orihara et al. 2012b). The nuclear multi-locus combined phylogeny shows that the sequestrate genera in the leccinoid clade are not monophyletic (Fig. 3). In contrast, the overall morphology between the two boletoid genera, *Leccinum* and *Leccinellum*, is similar (Den Bakker & Noordeloos 2005). Unfortunately, the phylogenetic placement of *Leccinellum* in the leccinoid clade has not been settled and the placement of *Chamonixia* as the earliest diverging lineage in the clade is only moderately supported (Fig. 3). Nonetheless, given that the phylogenetic analysis is consistent with the morphological differences among the sequestrate genera and the fact that the dominant fruitbody morphology in *Boletaceae* is the boletoid form (Binder & Hibbett 2006, Nuhn et al. 2013), these results suggest that the *Chamonixia*, *Octaviania*, and *Rossbeevera*/*Turmalinea* lineages evolved independently from different boletoid ancestors in the leccinoid clade.

Unfortunately, the multi-locus phylogenies in this study did not clarify the sister clade to the leccinoid clade (Fig. 2, 3) so we were unable to definitively determine the sequence of morphological changes that may have occurred during the evolution of this group. Recently, Wu et al. (2014) proposed several subfamilies across the *Boletaceae* based on nuclear multi-gene (nLSU, *EF-1 α* , *RPB1*, and *RPB2*) analyses. Among the proposed subfamilies was the *Leccinoideae*, which includes the genera of the leccinoid clade. Our phylogenetic analyses did not recover *Leccinoideae* but this is likely due to the difference of loci included in the combined dataset. Instead, two genera in the *Leccinoideae* (i.e., *Borofutus* and *Spongiforma*) were resolved in a monophyletic clade that included *Porphyrellus porphyrosporus*, which was treated as a member of

the *Boletoideae* in Wu et al. (2014). This suggests a need to re-evaluate the phylogenetic entity of the *Leccinoideae* based on different loci and more inclusive boletoid and sequestrate taxa. The addition of other DNA loci such as *RPB1* and *RPB2* will also help to resolve the generic relationships within the leccinoid clade more definitively.

The phylogenetic analyses also revealed a number of new species-level sequestrate lineages within *Rossbeevera* and *Turmalinea* with robust statistical support. Accordingly, we propose two new *Rossbeevera* species and four new species and one new subspecies of *Turmalinea*. The description of these new taxa almost doubles the number of species within the *Rossbeevera*-*Turmalinea* lineage, suggesting that this group is likely diverse and ecologically important in East Asia, Southeast Asia, and Australasia despite the fact that this lineage was only recently recognized (Lebel et al. 2012a, b). So far, *Turmalinea* accommodates only a few species (4 spp.) compared to *Rossbeevera* (10 spp.), and *Octaviania* (c. 30 spp.), but the long branches in the multi-gene phylogenies (Fig. 2, 3) imply that there are more undescribed species yet to be discovered. It is also possible, however, that the long branches are the result of extinction of ancestral species. Collecting surveys of sequestrate fungi across extensive areas in East Asia will give further insight into the diversity of *Turmalinea*.

While *Turmalinea* spp. are presently known only from East Asia (e.g., China and Japan), species of *Rossbeevera* have also been reported from Australasia and Southeast Asia (Lebel et al. 2012a, Orihara et al. 2012a, Vernes & Lebel 2011). Orihara et al. (2012a) and this study (Fig. 2, 3) agree that the Chinese species *R. yunnanensis* forms the basal branch within *Rossbeevera*. Based on these results we postulate that the genera *Turmalinea* and *Rossbeevera* may have originated in China or SE Asia and then migrated independently into Japan (including the Ryukyu Archipelago).

Similarly, all the phylogenies shown in this study suggest that the Australasian *Rossbeevera* species diversified relatively recently and that they probably migrated from Asia only once. Since sequestrate fungi are thought to rely on animal mycophagy for spore dispersal (Claridge & May 1994, Fogel & Trappe 1978, Maser 1978, Maser et al. 2008, Vernes & Dunn 2009), long-distance spore dispersal over ocean barriers would seem challenging. However, a biogeographic study by Hosaka et al. (2008) demonstrated that intercontinental, overseas dispersal has occurred separately in at least three truffle-like genera in the Hysterangiales, suggesting that overseas dispersal of truffles may be more common than previously thought. Field observations of truffle consumption by mammals indicate that *Rossbeevera* species are highly sought after as food. For example, *Rossbeevera* spores are among the most common spore types found in a diverse range of small Australian mammals (Lebel unpubl. data) and *Rossbeevera* spores have also been documented in mycophagous mammals from Papua New Guinea (Vernes & Lebel 2011). These observations suggest that intercontinental migration of *Rossbeevera* from Asia to Australasia may have been facilitated by mycophagous animals.

The sister sequestrate genera, *Turmalinea* and *Rossbeevera*, have several characteristics in common, including basidiospores with longitudinal ridges and fruitbodies that turn bluish upon bruising or exposure to air. However, *Turmalinea* species have firm, rubbery fruitbodies with a pulvinate sterile base and basidiospores with 5–10 longitudinal ridges whereas *Rossbeevera* species generally have softer fruitbodies with a reduced stipe-columella and basidiospores with 3–5 longitudinal ridges. In addition, three of the four *Turmalinea* species have brightly coloured, pinkish or yellow fruitbodies with yellow to orange rhizomorphs, whereas all *Rossbeevera* species have whitish to greyish white fruitbodies (Fig. 7). The one exceptional species

within *Turmalinea*, the earliest diverging species *T. mesomorpha*, forms whitish fruitbodies with bluish discolouration similar to species of *Rossbeevera*. This parsimoniously suggests that the ancestor of the two genera had a whitish sequestrate fruitbody with bluish discolouration and longitudinally ridged basidiospores as synapomorphies.

Although significantly supported in the phylogenetic analyses, it is difficult to infer close evolutionary relationships between bolete genera (i.e., *Leccinum* and *Leccinellum*) and sequestrate genera (i.e., *Rossbeevera*, *Turmalinea*, *Octaviania*, and *Chamonixia*) in the leccinoid clade based on morphology. For example, basidiospores of *Leccinellum* and *Leccinum* are smooth and colourless to pale brown, whereas those of the sequestrate taxa in *Rossbeevera*, *Turmalinea*, *Chamonixia*, and *Octaviania* are distinctly ornamented and brown to blackish brown. In addition, the epigeous boletoid taxa in the leccinoid clade have cheilo- and pleurocystidia in their tissues (Den Bakker & Noordeloos 2005) while the sequestrate taxa generally lack cystidia. The only distinct character that unites these genera is the reddish or bluish discolouration of fruitbodies, but this feature can also be found widely across both sequestrate and epigeous boletoid taxa in the *Boletaceae*. Therefore, we suggest that the evolution of dark pigmentation and enhanced ornamentation of basidiospores as well as the loss of cystidia are likely features that are selected for during the transition from boletoid to sequestrate fruiting form in the leccinoid clade. Future analyses using phylogenetic analysis in conjunction with molecular dating should examine the relationships between the micro- and macroscopic morphologies across the *Boletales* and particularly within poorly resolved groups within *Boletaceae*.

Interpreting evolutionary history in light of topological discord among phylogenies

The single-locus and combined phylogenies showed considerable topological discord at various degrees of divergence within *Rossbeevera*. The three single-locus nuclear trees exhibit different patterns of divergence among Japanese *Rossbeevera* spp. (Fig. 1). This topological incongruence can be explained by deep coalescence or incomplete lineage sorting (ILS) (Madison 1997). If this is true then sequences of ITS, nLSU, and *EF-1 α* were divergent in the ancestral *Rossbeevera* species before speciation events that led to the extant Japanese and Australasian *Rossbeevera* spp. The *BEAST analysis estimates a Bayesian species tree that accounts for effects of ILS under the multispecies coalescent model (Heled & Drummond 2010). Most conflicting topologies in the three nuclear gene trees were not satisfactorily reconciled in the *BEAST species tree based on the three loci, but the sister relationship between *R. eucyanea* and *R. cryptocyanea* was strongly supported by the *BEAST species tree (Fig. 2). These results suggest that gene trees based on other loci may mislead interpretations of the relationship between the two species. In addition, although most species-level relationships in *Rossbeevera* were strongly supported in the combined phylogeny (Fig. 3), the species tree analysis suggests that these internal relationships must be viewed critically in light of the incongruence between the various datasets.

We also compared the phylogeny based on three nuclear loci (ITS, nLSU, and *EF-1 α*) with an alternative topology based on two mitochondrial loci (*ATP6* and mtSSU) (Fig. 5). The nuclear phylogeny showed no obvious phylogeographic divergence within individual taxa. In contrast, the mitochondrial tree showed molecular divergence that unexpectedly followed patterns of geography rather than morphology. The case was particularly striking within the Australasian *Rossbeevera* species where we detected little differentiation between species based on the three nuclear loci. In contrast, the mitochondrial genes largely

exhibited a pattern of isolation by distance with geographically distant specimens also being genetically distant. Similar patterns were apparent in several species of Japanese *Rossbeevera* and *Turmalinea* (Fig. 5). Specimens of *R. griseovelutina* show considerable infraspecific divergence in the nuclear phylogeny. Specimens collected from western Honshu (the mainland of Japan) formed a single, homogenous clade based on the mitochondrial dataset whereas specimens from eastern Honshu and Amami-oshima Island (c. 600 km from Honshu) were genetically unique and more closely related to each other. In *T. persicina*, the nuclear phylogeny did not exhibit any obvious phylogeographic pattern, but the mitochondrial phylogeny suggested that specimens from Kyushu were slightly divergent from other Honshu specimens. These findings indicate that the infraspecific lineages in the genus *Rossbeevera* (including the Australasian species complex) may not be reproductively isolated, and that the infraspecific divergences in the mitochondrial genes are correlated to phylogeographic divergence rather than morphological and ecological differences.

Disagreement between the phylogenetic signals in nuclear vs mitochondrial loci have been documented for epigeous fungal genera and families such as the saprobic genus *Sparassis* (Polyporales) (Dai et al. 2006), ectomycorrhizal genus *Strobilomyces* (Boletales) (Sato et al. 2007, Sato & Murakami 2008), and the *Clavicipitaceae*, which includes fungi with diverse trophic modes (Sung et al. 2007). However, studies of these fungi did not detect any obvious biogeographic pattern in the diversification of mitochondrial loci (*ATP6* and/or *COX3* genes). It is possible that the unique ecological constraints imposed on sequestrate fungi (e.g. belowground fruiting, lack of active spore dispersal) may be correlated with geographical divergence in the mitochondrial phylogeny, but more data and comparisons with additional sequestrate taxa and related epigeal taxa are clearly needed to resolve this question.

The comparison between the nuclear and mitochondrial phylogenies also revealed divergent topological patterns within infraspecific lineages of *Rossbeevera*. One *R. griseovelutina* specimen (TNS-F-36991) is resolved in the *R. griseovelutina* lineage 2 based on the nuclear markers (ITS, nLSU, *EF-1 α*) but is grouped together with the members of the *R. griseovelutina* lineage 1 based on the mitochondrial markers (*ATP6* and mtSSU) (Fig. 5). Since the other specimens of *R. griseovelutina* lineage 2 in the nuclear tree showed phylogenetic affinity in the mitochondrial tree, ILS between the two lineages is not likely. This conflict could be more reasonably explained by introgression of mitochondrial genes because both *R. griseovelutina* lineage 1 and lineage 2 are found in western Honshu where lineage 1 occurs in evergreen *Castanopsis* forests and lineage 2 is found in nearby deciduous *Fagus-Quercus* forests. It is possible that distribution of the two lineages overlaps in some areas in western Honshu, and this could cause the introgression of mitochondrial genes. It is not obvious, however, why the two individuals of the lineages 1 and 2 collected from Amami-oshima Island and Eastern Honshu, which are geographically distant from one another (c. 1 200 km), have almost identical *ATP6* and mtSSU sequences. Given that the mitochondrial sequences of *Rossbeevera* tend to reflect geographic distance, transoceanic spore dispersal as well as gene introgression would be necessary to explain these topologies. The precise pattern of migration cannot be concluded thus far due to insufficient samples. However, additional sampling throughout the region might help to clarify the process of transoceanic spore dispersal of truffles in the future.

Several studies on the evolutionary biology of fungi and animals have detected similar incongruence between nuclear and mitochondrial datasets. Dai et al. (2006) demonstrated that three *Sparassis* species distinct in the nuclear phylogeny

shared identical mitochondrial *ATP6* sequences. The authors inferred that this was due to clonal inheritance within the partly overlapping populations. Similarly, Robinson et al. (2001) found remarkably low divergence in *ATP6* of *Agaricus bisporus* isolates with different mitochondrial haplotypes but they did not mention the possibility of ILS or introgression. Peters et al. (2007) examined the mitochondrial paraphyly between gadwalls and falcated ducks and rejected the hypothesis of ILS based mainly on incongruence between the divergence time of the two species estimated by nuclear introns and mtDNA genes. Similar approaches and addition of sequences of *R. griseovelutina* may offer further insights about evaluation of ILS and introgression in *Rossbeevera*.

Although ILS seems unlikely in the case of the topological conflict within *R. griseovelutina*, it seems probable that ILS does account for the topological incongruence within *R. paracyanea* (Fig. 5). Both infraspecific lineages of *R. paracyanea* were from the same region (western Honshu, Japan), and Fig. 5 shows the infraspecific divergence in the mitochondrial two-locus phylogeny is deeper compared to that in the nuclear three-locus phylogeny. Although we cannot conclude any historical event that affects the topological incongruence based only on the small number of *R. paracyanea* samples, the parsimonious explanation is incongruence caused by ILS derived from mitochondrial polymorphism within the ancestor of the extant *R. paracyanea* lineages. Considering these cases of putative ILS between the nuclear and mitochondrial loci and the likely ILS found among the nuclear single-locus trees, it seems that ILS is not a rare event in this group of fungi. Furthermore, the frequent polymorphism in the nuclear loci of the Australasian *Rossbeevera* 'spp.' may be another example of the ongoing process of lineage sorting (Fig. 1).

Similar topological patterns to *R. paracyanea* were recovered in the relationship between *R. cryptocyanea* lineages 1 and 2 (Fig. 5). In this case, however, both ILS and introgression are possible causes of the topological discordance because the pattern of divergence in the mitochondrial tree also reflected geographical distances among the specimens. The distance between the two localities, Kakeroma and Amami-oshima Islands, is c. 15 km, whereas Ishigaki Island is c. 650 km distant from Amami-oshima Island, and the Kerama Gap, which is known as a faunal gap of many terrestrial animals, crosses between them (Ota 1998). Therefore, it is also possible that the two different infraspecific lineages of *R. cryptocyanea* occurred sympatrically and that this caused introgression of mitochondrial genes.

Overall, the analysis of nuclear vs mitochondrial loci revealed that genetic distances in the mitochondrial tree generally correspond to geographic distance within each species-level lineage of *Rossbeevera* and *Turmalinea*. While some topological conflicts within *Rossbeevera* species may be the results of recent gene introgression, other conflicts strongly suggest the possibility of incomplete lineage sorting between closely related lineages. These examples indicate that careful, multifaceted characterization using both morphological and phylogeographical methods with nuclear and mitochondrial datasets is the key to delimit boundaries between infrageneric taxa. It is also possible that these types of complex evolutionary histories may be frequently overlooked in phylogenetic studies of many other fungal taxa due to insufficient sampling of individuals and due to the lack of precise topological comparisons between phylogenies based on different loci.

Minisatellite-like insertion in ITS2 as a DNA barcode marker

The ITS region has recently been adopted as the official molecular barcode for fungi (Chase & Fay 2009, Schoch et al. 2012). Although most fungi in Basidiomycota have an ITS region (ITS1-5.8S-ITS2) that is approximately 500–650 nucleotides,

PCR amplicons of ITS in *Rossbeevera* and *Turmalinea* species are remarkably large (e.g., ITS in *T. persicina* is about 1 100 base pairs). The extra length of this region is due to the presence of a minisatellite-like insertion within ITS2 (Table 2). ITS minisatellites are rare in fungi, but Den Bakker et al. (2004) reported that species of *Leccinum*, a species-rich bolete genus in the leccinoid clade, usually contain minisatellite-like insertions in ITS1. They demonstrated that the minisatellite-like insertions were highly divergent among infraspecific lineages of *Leccinum* and therefore not usable as a phylogenetic marker at or above species level. Orihara et al. (2012b) briefly mentioned the presence of insertions in the ITS2 region of species in *Octaviania* subg. *Fulvoglobus*, but did not characterize the DNA sequences of the insertions.

In this study we used the Automatic Barcode Gap Discovery (ABGD) software (Puillandre et al. 2012), to infer species boundaries within *Rossbeevera* and *Turmalinea*. The barcode gap analysis and ML phylogeny clearly showed that the minisatellite-like insertions of *Rossbeevera* and *Turmalinea* were highly conserved at the subspecies-, species- and genus levels and that these minisatellites have higher resolution in discriminating the boundary between intergeneric-level, infraspecific-level, and interspecific-level divergence than the rest of the ITS region (Fig. 6). The Australasian *Rossbeevera* spp., however, were not partitioned at the species-level boundary estimated by the analysis (Fig. 6c). This suggests that these previously described species are likely geographic variants that may still be in the process of speciation, despite the fact that several specimens from different regions of Australasia show remarkable morphological divergence (Lebel et al. 2012a).

Although the exact origin of these ITS insertions are unclear, it is likely that they originated within the leccinoid clade since no other group in the Boletales appear to have them. Although we have not characterized the structure and function of the minisatellite-like insertions, the insertion sequences of *Rossbeevera* and *Turmalinea* are highly informative and can thus be used efficiently for DNA barcoding of fruitbodies or environmental sequences. We caution, however, that the extended ITS length in *Rossbeevera* and *Turmalinea* may actually reduce the likelihood that these DNA sequences will be recovered from environmental samples since longer fragments are sometimes discriminated against in mixed pools of DNA (Huber et al. 2009, Bellemain et al. 2010).

Conclusions

Our finding of a new sequestrate genus, *Turmalinea*, reinforces the fact that the leccinoid clade is remarkably rich in sequestrate fungi. The nuclear three-locus phylogenies strongly supported the distinctness of the four new species and one new subspecies of *Turmalinea* as well as the two new species of *Rossbeevera* despite the fact that precise infrageneric relationships within *Rossbeevera* remain unclear. Topological comparison between nuclear and mitochondrial phylogenies documented significant infraspecific biogeographical diversification of two mitochondrial loci in the Australasian *Rossbeevera* species but very low differentiation in nuclear loci. Pairwise comparison among nuclear and mitochondrial trees further suggested that mtDNA introgression and ILS have occurred within multiple inter- and infraspecific lineages of *Rossbeevera*. Finally, we used the recently developed barcode gap analysis, ABGD, to demonstrate that the minisatellite-like insertion found in the ITS2 of *Rossbeevera* and *Turmalinea* is highly informative for identifying infra- and interspecific and intergeneric divergence. Although the ABGD approach has only rarely been used to delimit species of fungi, our results suggest that this method holds great promise for future studies of molecular identification in fungi, particularly since the ITS region has been adopted as

the official fungal barcode region (Chase & Fay 2009, Schoch et al. 2012).

In a few lineages of *Rossbeevera* and *Turmalinea*, we were not able to include multiple infraspecific OTUs in the phylogenetic analyses because these sequestrate fungi are mostly hypogeous and they are rarely collected. Moreover, we know of no DNA sequences from *R. mucosa* or *R. bispora* because all of the available specimens were collected too long ago and some of them are fragmentary. We hope that in the near future comprehensive taxon sampling of both epigeous and sequestrate leccinoid taxa will reveal more precise phylogenetic and phylogeographic relationships and evolutionary processes.

Acknowledgements We are grateful to Michael A. Castellano, James M. Trappe, Josef W. Spatafora, Alija Mujic, Kentaro Hosaka, and Giovanni Pacioni for facilitating access to herbarium specimens. We especially thank Muneyuki Ohmae for his useful suggestions on this study and providing specimens. Konomi Yanaga and Shigeyuki Murakami kindly supported us to take SEM images of basidiospores. Jun-ichi Kikuchi, Hisako Inui, Minami Inui, Mitsuru Moriguchi, Shigeo Morimoto, Ayako Okuda, Takashi Sasa, Yoichi Sunada, and Kohei Yamamoto facilitated our fieldworks and helped with collecting. We also thank Akiko Kajiyama, Fumitaka Nagao, Yokin-no-Kai, Yuzo Kotera, Masaru Ohkubo, Atsuko Hadano, Eiji Hadano, Yasushi Kawaguchi, Mayumi Kawai, Shunsuke Matsuoka, Minoru Nakajima, Masahito Taniguchi, Hidehiko Ikeda for providing valuable specimens. Atsushi Nakajima helped the molecular experiments. The study was supported by the Grant-in-Aid for Institute for Fermentation, Osaka (IFO), Research Fellowships for Young Scientists (no. 21-6052) from the Japan Society for the Promotion of Science (JSPS), JSPS KAKENHI Grant-in-Aid for Young Scientists (B) (no. 25840149), and the Grant-in-Aid for the Global COE Program 'Advanced Utilization of Fungus/Mushroom Resources for Sustainable Society in Harmony with Nature' from the Ministry of Education, Culture, Sports, Science and Technology (MEXT) of Japan. Support for the participation of M.E. Smith was facilitated by the Institute for Food and Agriculture (IFAS) at University of Florida.

REFERENCES

Altschul SF, Madden TL, Schäffer AA, et al. 1997. Gapped BLAST and PSI-BLAST: a new generation of protein database search programs. *Nucleic Acids Research* 25: 3389–3402.

Aoki M. 1978. *Shima-shoro* [Gauteria sp.]. In: Aoki M (ed), Illustrations of Japanese mushrooms with colour prints, Japan: No.1020. In Japanese.

Arora D, Frank JL. 2014. Clarifying the butter Boletes: a new genus, *Butyriboletus*, is established to accommodate *Boletus* sect. *Appendiculati*, and six new species are described. *Mycologia* 106: 464–480.

Beever RE, Lebel T. 2014. Truffles of New Zealand: a discussion of bird dispersal characteristics of fruit bodies. *Auckland Botanical Journal* 6: 170–177.

Bellemain E, Carlsen T, Brochmann C, et al. 2010. ITS as an environmental DNA barcode for fungi: an in silico approach reveals potential PCR biases. *BMC Microbiology* 10: 189.

Benson G. 1999. Tandem repeats finder: a program to analyze DNA sequences. *Nucleic Acids Research* 27: 573–580.

Bessette AE, Roody W, Bessette AR. 2000. North American Boletes: A color guide to the fleshy pored mushrooms. Syracuse University Press, Syracuse, New York, USA.

Binder M, Hibbett DS. 2006. Molecular systematics and biological diversification of Boletales. *Mycologia* 98: 971–981.

Bouckaert R, Heled J, Kühnert D, et al. 2014. BEAST2: A software platform for Bayesian evolutionary analysis. *PLoS Computational Biology* 10: e1003537.

Bougher NL, Tommerup IC, Malajczuk N. 1993. Broad variation in developmental and mature fruitbody morphology of the ectomycorrhizal fungus *Hydnangium sublamellatum* sp. nov. bridges morphologically based generic concepts of *Hydnangium*, *Podohydnangium* and *Laccaria*. *Mycological Research* 97: 613–619.

Bruns TD, Fogel R, White TJ, et al. 1989. Accelerated evolution of a false-truffle from a mushroom ancestor. *Nature* 339: 140–142.

Bruns TD, Szaro TM, Gardes M, et al. 1998. A sequence database for the identification of ectomycorrhizal basidiomycetes by phylogenetic analysis. *Molecular Ecology* 7: 257–272.

Castillo-Ramírez S, Liu L, Pearl D, et al. 2010. Bayesian estimation of species trees: a practical guide to optimal sampling and analysis. In: Knowles LL, Kubatko LS (eds), Estimating species trees: practical and theoretical aspects: 15–33. Wiley-Blackwell, USA.

Castresana J. 2000. Selection of conserved blocks from multiple alignments for their use in phylogenetic analysis. *Molecular Biology and Evolution* 17: 540–552.

Chase MW, Fay MF. 2009. Barcoding of plants and fungi. *Science* 325: 682–683.

Claridge AW, May TW. 1994. Mycophagy among Australian mammals. *Australian Journal of Ecology* 19: 251–275.

Dai YC, Wang Z, Binder M, et al. 2006. Phylogeny and a new species of *Sparassis* (Polyporales, Basidiomycota): evidence from mitochondrial atp6, nuclear rDNA and rpb2 genes. *Mycologia* 98: 584–592.

Danks MA. 2011. The swamp wallaby *Wallabia bicolor*: a generalist browser as a key mycophagist. PhD thesis, University of New England, NSW, Australia.

Den Bakker HC, Gravendeel B, Kuyper TW. 2004. An ITS phylogeny of *Leccinum* and an analysis of the evolution of minisatellite-like sequences within ITS1. *Mycologia* 96: 112–118.

Den Bakker HC, Noordeloos ME. 2005. A revision of European species of *Leccinum* Gray and notes on extralimital species. *Persoonia* 18: 511–587.

Dentinger BT, Ammirati JF, Both EE, et al. 2010. Molecular phylogenetics of porcini mushrooms (*Boletus* section *Boletus*). *Molecular Phylogenetics and Evolution* 57: 1276–1292.

Dentinger BT, McLaughlin DJ. 2006. Reconstructing the Clavariaceae using nuclear large subunit rDNA sequences and a new genus segregated from *Clavaria*. *Mycologia* 98: 746–752.

Desjardin DE, Binder M, Roekring S, et al. 2009. *Spongiforma*, a new genus of gasteroid boletes from Thailand. *Fungal Diversity* 37: 1–8.

Desjardin DE, Wilson AW, Binder M. 2008. *Durianella*, a new gasteroid genus of boletes from Malaysia. *Mycologia* 100: 956–961.

Faith DP. 1992. Conservation evaluation and phylogenetic diversity. *Biological Conservation* 61: 1–10.

Faith DP, Baker AM. 2006. Phylogenetic diversity (PD) and biodiversity conservation: some bioinformatics challenges. *Bioinformatics* 2: 121–128.

Fogel R, Trappe JM. 1978. Fungal consumption (mycophagy) by small animals. *Northwest Science* 52: 1–31.

Frank JL, Anglin S, Carrington EM, et al. 2009. Rodent dispersal of fungal spores promotes seedling establishment away from mycorrhizal networks on *Quercus garryana*. *Botany* 87: 821–829.

Galtier N, Gouy M, Gautier C. 1996. SEAVIEW and PHYLO_WIN: Two graphic tools for sequence alignment and molecular phylogeny. *Computer Applications in the Biosciences* 12: 543–548.

Gardes M, Bruns TD. 1993. ITS primers with enhanced specificity for basidiomycetes: application to the identification of mycorrhizae and rusts. *Molecular Ecology* 2: 113–118.

Gelardi M, Simonini G, Ercole E, et al. 2014. *Alessioporus* and *Pulchroboletus* gen. nov. (Boletaceae, Boletineae), two novel genera for *Xerocomus ichnusanus* and *X. roseoalbidus* from the European Mediterranean basin: molecular and morphological evidence. *Mycologia* 106: 1168–1187.

Geyer CJ. 1991. Markov chain Monte Carlo maximum likelihood. In: Keramidas EM (eds), Computing science and statistics. Proceedings of the 23rd symposium on the interface: 156–163. Fairfax Station, Interface Foundation, USA.

Hall TA. 1999. BioEdit: a user-friendly biological sequence alignment editor and analysis program for Windows 96/98/NT. *Nucleic Acids Symposium Series* 41: 95–98.

Halling RE, Nuhn M, Fechner NA, et al. 2012a. *Sutorius*: a new genus for *Boletus eximius*. *Mycologia* 104: 951–961.

Halling RE, Nuhn M, Osmundson T, et al. 2012b. Affinities of the *Boletus* chromapes group to *Royoungia*. *Australian Systematic Botany* 25: 418–431.

Heled J, Drummond AJ. 2010. Bayesian inference of species trees from multilocus data. *Molecular Biology and Evolution* 27: 570–580.

Hibbett DS. 2004. Trends in morphological evolution in homobasidiomycetes inferred using maximum likelihood: A comparison of binary and multistate approaches. *Systematic Biology* 53: 889–903.

Hibbett DS, Pine EM, Langer E, et al. 1997. Evolution of gilled mushrooms and puffballs inferred from ribosomal DNA sequences. Proceedings of the National Academy of Sciences, USA 94: 12002–12006.

Hibbett DS, Tsuneda A, Murakami S. 1994. The sectoid form of *Lentinus tigrinus*: genetics and development of a fungal morphological innovation. *American Journal of Botany* 81: 466–478.

Hosaka K, Bates ST, Beever RE, et al. 2006. Molecular phylogenetics of the gomphoid-phalloid fungi with an establishment of the new sub-class Phallomycetidae and two new orders. *Mycologia* 98: 949–959.

Hosaka K, Castellano M, Spatafora JW. 2008. Biogeography of Hysterangiales (Phallomycetidae, Basidiomycota). *Mycological Research* 112: 448–462.

Hosen MI, Feng B, Wu G, et al. 2012. *Borofutus*, a new genus of Boletaceae from tropical Asia: phylogeny, morphology and taxonomy. *Fungal Diversity* 58: 215–226.

- Huber JA, Morrison HG, Huse SM, et al. 2009. Effect of PCR amplicon size on assessments of clone library microbial diversity and community structure. *Environmental Microbiology* 11: 1292–1302.
- Katoh K, Standley DM. 2013. MAFFT Multiple Sequence Alignment Software Version 7: Improvements in performance and usability. *Molecular Biology and Evolution* 30: 772–780.
- Kendrick B. 1992. *The Fifth Kingdom*, 2nd ed. Mycologue Publications, Ontario, Canada.
- Kimura M. 1980. A simple method for estimating evolutionary rates of base substitutions through comparative studies of nucleotide sequences. *Journal of Molecular Evolution* 16: 111–120.
- Kretzer AM, Bruns TD. 1999. Use of *atp6* in fungal phylogenetics; an example from the Boletales. *Molecular Phylogenetics and Evolution* 13: 483–492.
- Læssøe T, Hansen K. 2007. Truffle trouble: what happened to the Tuberales? *Mycological Research* 111: 1075–1099.
- Larsson K-H, Larsson E, Kõljalg U. 2004. High phylogenetic diversity among corticioid basidiomycetes. *Mycological Research* 108: 983–1002.
- Lebel T, Castellano MA, Beever RE. 2015. Cryptic diversity in the sequestrate genus *Stephanospora* (Stephanosporaceae: Agaricales) in Australasia. *Fungal Biology* 119: 201–228.
- Lebel T, Orihara T, Maekawa N. 2012a. The sequestrate genus *Rosbeeva* T. Lebel & Orihara gen. nov. (Boletaceae) from Australasia and Japan: new species and new combinations. *Fungal Diversity* 52: 49–71.
- Lebel T, Orihara T, Maekawa N. 2012b. Erratum to: The sequestrate genus *Rosbeevera* T. Lebel & Orihara gen. nov. (Boletaceae) from Australasia and Japan: new species and new combinations. *Fungal Diversity* 52: 73.
- Lebel T, Syme A. 2012. Sequestrate species of *Agaricus* and *Macrolepiota* from Australia: new species and combinations and their position in a calibrated phylogeny. *Mycologia* 104: 496–520.
- Li Y-C, Li F, Zeng N-K, et al. 2014. A new genus *Pseudoaustroboletus* (Boletaceae, Boletales) from Asia as inferred from molecular and morphological data. *Mycological Progress* 13: 1207–1216.
- Maddison WP. 1997. Gene trees in species trees. *Systematic Biology* 46: 523–536.
- Maddison WP, Knowles LL. 2006. Inferring phylogeny despite incomplete lineage sorting. *Systematic Biology* 55: 21–30.
- Maser C, Claridge AW, Trappe J. 2008. *Trees, truffles, and beasts: How forests function*. Rutgers University Press, USA.
- Maser C, Trappe JM, Nussbaum RA. 1978. Fungal-small mammal interrelationships with emphasis on Oregon coniferous forests. *Ecology* 59: 799–809.
- Miettinen O, Larsson E, Sjökvist E, et al. 2012. Comprehensive taxon sampling reveals unaccounted diversity and morphological plasticity in a group of dimorphic polypores (Polyporales, Basidiomycota). *Cladistics* 28: 251–270.
- Nuhn ME, Binder M, Taylor AF, et al. 2013. Phylogenetic overview of the Boletineae. *Fungal Biology* 117: 479–511.
- Nylander JAA. 2004. MrModeltest v2. Program distributed by the author. Evolutionary Biology Centre, Uppsala University Sweden.
- Orihara T, Sawada F, Ikeda S, et al. 2010. Taxonomic reconsideration of a sequestrate fungus, *Octaviania columellifera*, with the proposal of a new genus, *Heliogaster*, and its phylogenetic relationships in the Boletales. *Mycologia* 102: 108–121.
- Orihara T, Smith ME, Ge Z-W, et al. 2012a. *Rosbeevera yunnanensis* (Boletaceae, Boletales), a new sequestrate species from southern China. *Mycotaxon* 120: 139–147.
- Orihara T, Smith ME, Shimomura N, et al. 2012b. Diversity and systematics of the sequestrate genus *Octaviania* in Japan: two new subgenera and eleven new species. *Persoonia* 28: 85–112.
- Ota H. 1998. Geographic patterns of endemism and speciation in amphibians and reptiles of the Ryukyu Archipelago, Japan, with special reference to their paleogeographical implications. *Researches on Population Ecology* 40: 189–204.
- Pegler DN, Young TWK. 1989. *Rhodactina himalayensis* gen. et sp. nov. (Gautieriaceae) from India. *Opera Botanica* 100: 201–206.
- Peintner U, Bougher NL, Castellano MA, et al. 2001. Multiple origins of sequestrate fungi related to *Cortinarius* (Cortinariaceae). *American Journal of Botany* 88: 2168–2179.
- Percudani R, Trevisi A, Zambonelli A, et al. 1999. Molecular phylogeny of truffles (Pezizales: Terfeziaceae, Tuberales) derived from nuclear rDNA sequence analysis. *Molecular Phylogenetics and Evolution* 13: 169–180.
- Peters JL, Zhuravlev Y, Fefelov I, et al. 2007. Nuclear loci and coalescent methods support ancient hybridization as cause of mitochondrial paraphyly between gadwall and falcated duck (*Anas spp.*). *Evolution* 61: 1992–2006.
- Pine EM, Hibbett DS, Donoghue MJ. 1999. Phylogenetic relationships of cantharelloid and clavarioid Homobasidiomycetes based on mitochondrial and nuclear rDNA sequences. *Mycologia* 91: 944–963.
- Puillandre N, Lambert A, Brouillet S, et al. 2012. ABGD, Automatic Barcode Gap Discovery for primary species delimitation. *Molecular Ecology* 21: 1864–1877.
- Rambaut A, Drummond AJ. 2009. Tracer v1.5. Available from <http://tree.bio.ed.ac.uk/software/tracer/>.
- Rehner SA, Buckley E. 2005. A *Beauveria* phylogeny inferred from nuclear ITS and EF1- α sequences: evidence for cryptic diversification and links to *Cordyceps* teleomorphs. *Mycologia* 97: 84–98.
- Robison MM, Chiang B, Horgen PA. 2001. A phylogeny of the genus *Agaricus* based on mitochondrial *atp6* sequences. *Mycologia* 93: 30–37.
- Ronquist F, Huelsenbeck JP. 2003. MrBayes 3: Bayesian phylogenetic inference under mixed models. *Bioinformatics* 19: 1572–1574.
- Sato H, Murakami N. 2008. Reproductive isolation among cryptic species in the ectomycorrhizal genus *Strobilomyces*: population-level CAPS marker-based genetic analysis. *Molecular Phylogenetics and Evolution* 48: 326–334.
- Sato H, Yumoto T, Murakami N. 2007. Cryptic species and host specificity in the ectomycorrhizal genus *Strobilomyces* (Strobilomyceataceae). *American Journal of Botany* 94: 1630–1641.
- Schoch CL, Seifert KA, Huhndorf S, et al. 2012. Nuclear ribosomal internal transcribed spacer (ITS) region as a universal DNA barcode marker for Fungi. *Proceedings of the National Academy of Sciences, USA* 109: 6241–6246.
- Silvestro D, Michalak I. 2012. raxmlGUI: a graphical front-end for RAxML. *Organism Diversity and Evolution* 12: 335–337.
- Stamatakis A. 2006. RAxML-VI-HPC: maximum likelihood-based phylogenetic analyses with thousands of taxa and mixed models. *Bioinformatics* 22: 2688–2690.
- Sung GH, Sung JM, Hywel-Jones NL, et al. 2007. A multi-gene phylogeny of Glavicipitaceae (Ascomycota, Fungi): identification of localized incongruence using a combinational bootstrap approach. *Molecular Phylogenetics and Evolution* 44: 1204–1223.
- Thiers HD. 1984. The secotioid syndrome. *Mycologia* 76: 1–8.
- Thompson JD, Gibson TJ, Plewniak F, et al. 1997. The Clustal X windows interface: flexible strategies for multiple sequence alignment aided by quality analysis tools. *Nucleic Acids Research* 25: 4876–4882.
- Trappe JM, Castellano MA, Halling RE, et al. 2013. Australasian sequestrate fungi 18: *Soliococcus polychromus* gen. & sp. nov., a richly colored, tropical to subtropical, hypogeous fungus. *Mycologia* 105: 888–895.
- Trappe JM, Molina R, Luoma D, et al. 2009. Diversity, ecology, and conservation of truffle fungi in forests of the Pacific Northwest. General Technical Reports PNW-GTR-772, U.S. Department of Agriculture, Forest Service, Pacific Northwest Research Station, Oregon, USA.
- Vernes K, Dunn L. 2009. Mammal mycophagy and fungal spore dispersal across a steep environmental gradient in eastern Australia. *Australian Ecology* 34: 69–76.
- Vernes K, Lebel T. 2011. Truffle consumption by New Guinea forest wallabies. *Fungal Ecology* 4: 270–276.
- Vilgalys R, Hester M. 1990. Rapid genetic identification and mapping of enzymatically amplified ribosomal DNA from several *Cryptococcus* species. *Journal of Bacteriology* 172: 4238–4246.
- White TJ, Bruns T, Lee S, et al. 1990. Amplification and direct sequencing of fungal ribosomal RNA genes for phylogenetics. In: Innis MA, Gelfand DH, Sninsky JJ, et al. (eds), *PCR Protocols: a guide to methods and applications*: 315–322. Academic Press, USA.
- Wilson AW, Binder M, Hibbett DS. 2011. Effects of gasteroid fruiting body morphology on diversification rates in three independent clades of fungi estimated using binary state speciation and extinction analysis. *Evolution* 65: 1305–1322.
- Wu G, Feng B, Xu J, et al. 2014. Molecular phylogenetic analyses redefine seven major clades and reveal 22 new generic clades in the fungal family Boletaceae. *Fungal Diversity* 69: 93–115.
- Yanaga K, Maekawa N, Shimomura N, et al. 2012. Use of ionic liquid in fungal taxonomic study of ultrastructure of basidiospore ornamentation. *Mycological Progress* 11: 343–347.
- Yang Z. 1994. Maximum likelihood phylogenetic estimation from DNA sequences with variable rates over sites: Approximate methods. *Journal of Molecular Evolution* 39: 306–314.
- Yang ZL, Trappe JM, Binder M, et al. 2006. The sequestrate genus *Rhodactina* (Basidiomycota, Boletales) in northern Thailand. *Mycotaxon* 96: 133–140.
- Yoshimi S. [Sakuma D. ed.] 2009. Yoshimi-Shoichi hukkin-rui siryo-syu (Unpublished works on gasteromycetes by Sho-ichi Yoshimi). Kansai Mycological Club, Japan. In Japanese.
- Yoshimi S, Doi Y. 1989. Japanese gasteromycetes notes (1). *Memoirs of the National Science Museum, Tokyo* 22: 29–41. In Japanese with English summary.
- Zeng N-K, Wu G, Li Y-C, et al. 2014. *Crocinoletus*, a new genus of Boletaceae (Boletales) with unusual boletocrocin polyene pigments. *Phytotaxa* 175: 133–140.